UNIVERSITY OF CALIFORNIA SAN DIEGO

Measuring Electrical Charge and Molecular Interaction at Solid/Liquid Interface from Integrated Transient Induced Molecular Electronic Signal (i-TIMES)

A dissertation submitted in partial satisfaction of the
requirements for the degree
Doctor of Philosophy

in

Chemical Engineering

by

Ping-Wei Chen

Committee in charge:

Professor Yu-Hwa Lo, Chair
Professor Jinhye Bae
Professor Yi Chen
Professor James Friend
Professor Ratnesh Lal
Professor Andrea Tao

2020

The Dissertation of Ping-Wei Chen is approved, and it is acceptable in quality and form for publication on microfilm and electronically:

_____

_____

_____

_____

_____

_____

Chair

University of California, San Diego

2020

DEDICATION

To my family and friends.

TABLE OF CONTENTS

LIST OF FIGURES

LIST OF TABLES

ACKNOWLEDGMENTS

First of all, I would like to sincerely thank my advisor, Professor Yu-Hwa Lo, for his guidance, patience and support not only as an advisor but also as a mentor. His dedication to research, critical thinking and problem solving are the most important things I have learned throughout my Ph.D. I would like to thank my committee members, Professor Andrea Tao, Professor Yi Chen, Professor Jinhye Bae, Professor James Friend, Professor Ratnesh Lal, Professor Donald Sirbuly and Professor Justin Opatkiewicz for their time and help on my research project and my dissertation. Without their insightful comments and valuable suggestions, my research would not be accomplished.

Next, I need to thank my collaborator, Fumin Shi and Bo Bi, who provide rich information and support on the knowledge related to biomolecular. I appreciate the help from all of my colleagues in University of California San Diego, Chi-Yang Tseng, Tiantian Zheng, Cai Wei, Alex Zheng, Tony Yen, Yi-Huan Tsai, Yu-Jui Chiu, Yu-Hsin Liu and Tsung-Feng Wu. Their great help and valuable discussion of the research makes my research wider from various perspectives.

I would also like to thank all my friends who were there with me during my Ph.D. Moreover, I need to thank my teacher from Taiwan, Yuan-Jung Chen, who always encourages me to pursue my goal without hesitation. Last but not least, I would like to thank my parents, Chung-Hsiung Chen and Chin-Hong Ko, and my brother,

Ping-Yen Chen, who were with me every step of this journey. Without their support, I could not possibly finish my Ph.D.

The material in this dissertation is based on the following papers which are either published or under final process for publication.

Portions of Chapter 2 is a reprint of the materials as they appear in *Scientific Reports*, 2019 and *Analytical Chemistry*, 2019. Ping-Wei Chen, Chi-Yang Tseng, Fumin Shi, Bo Bi, Yu-Hwa Lo. Measuring Electric Charge and Molecular Coverage on Electrode Surface from Transient Induced Molecular Electronic Signal (TIMES). *Scientific Reports*, 2019, 9, 1-10 and Ping-Wei Chen, Chi-Yang Tseng, Fumin Shi, Bo Bi, Yu-Hwa Lo. Detecting Protein-Ligand Interaction from Integrated Transient Induced Molecular Electronic Signal (i-TIMES). *Analytical Chemistry*, 2019, accepted.

Portions of Chapter 3 is a reprint of the material as it appears in *Scientific Reports*, 2019. Ping-Wei Chen, Chi-Yang Tseng, Fumin Shi, Bo Bi, Yu-Hwa Lo. Measuring Electric Charge and Molecular Coverage on Electrode Surface from Transient Induced Molecular Electronic Signal (TIMES). *Scientific Reports*, 2019, 9, 1-10.

Part of Chapter 4 is a reprint of the material as it appears in *Analytical Chemistry*, 2019. Ping-Wei Chen, Chi-Yang Tseng, Fumin Shi, Bo Bi, Yu-Hwa Lo. Detecting Protein-Ligand Interaction from Integrated Transient Induced Molecular Electronic Signal (i-TIMES). *Analytical Chemistry.*, 2019, accepted.

The dissertation author was the first author of these papers.

Ping-Wei Chen

La Jolla, CA

February 2020

VITA

EDUCATION

2008 – 2012	Bachelor of Science, National Taiwan University, Taiwan
2013 – 2015	Master of Science, University of California San Diego, USA
2015 – 2020	Doctor of Philosophy, University of California San Diego, USA

FIELD OF STUDY

Chemical Engineering

PUBLICATIONS

Ping-Wei Chen, Chi-Yang Tseng, Fumin Shi, Bo Bi, Yu-Hwa Lo. Detecting Protein-Ligand Interaction from Integrated Transient Induced Molecular Electronic Signal (i-TIMES). *Analytical Chemistry*, 2019, accepted

Ping-Wei Chen, Chi-Yang Tseng, Fumin Shi, Bo Bi, Yu-Hwa Lo. Measuring Electric Charge and Molecular Coverage on Electrode Surface from Transient Induced Molecular Electronic Signal (TIMES). *Scientific Reports*, **9**, 1-10, 2019

Da Ying, **Ping-Wei Chen**, Chi-Yang Tseng, Yu-Hwa Lo, Drew A. Hall. A Sub-pA Current Front-End for Transient Induced Molecular Spectroscopy. *IEEE 2019 Symposium on VLSI Circuits*, C316-C317, 2019

Wei Cai, Edward Wang, **Ping-Wei Chen**, Yi-Huan Tsai, Lennart Langouche, Yu-Hwa Lo. A Microfluidic Design for Desalination and Selective Removal and Addition of Components in Biosamples. *Biomicrofluidics*, **13** (2), 024109, 2019

Tiantian Zhang, Tao Wei, Yuanyuan Han, Heng Ma, Mohammadreza Samieegohar, **Ping-Wei Chen**, Ian Lian, Yu-Hwa Lo. Protein-Ligand Interaction Detection with a Novel Method of Transient Induced Molecular Electronic Spectroscopy (TIMES): Experimental and Theoretical Studies. *ACS Central Science*, **2** (11), 834–842, 2016

Tony Yen, Tiantian Zhang, **Ping-Wei Chen**, Ti-Hsuan Ku, Ian Lian, Yu-Hwa Lo. Self-assembled nano-droplet microarray for ultrasensitive nucleic acid quantification. *ACS Nano*, **9** (11), 10655–10663, 2015

Ti-Hsuan Ku, Tiantian Zhang, Hua Luo, Tony M. Yen, **Ping-Wei Chen**, Yuanyuan Han, Yu-Hwa Lo. Nucleic acid apatamers: an emerging tool for biotechnology and biomedical sensing. *Sensors*, **15** (7), 16281-16313, 2015

PATENT

Yu-Hwa Lo, **Ping-Wei Chen,** Chi-Yang Tseng. Detection of liquid/solid interface properties and molecular interactions using Integrated Transient Induced Molecular Electronic Signal (i-TIMES), *US Patent*, under review

ABSTRACT OF THE DISSERTATION

Measuring Electrical Charge and Molecular Interaction at Solid/Liquid Interface from Integrated Transient Induced Molecular Electronic Signal (i-TIMES)

by

Ping-Wei Chen

Doctor of Philosophy in Chemical Engineering

University of California San Diego, 2020

Professor Yu-Hwa Lo, Chair

To determine the surface charge density near the electrode surface plays an important role in the studies related to biomedical device and bio-related surface reaction. This dissertation presents a technique, Integrated Transient Induced

Molecular Electronic Signal (i-TIMES) method, which is an extended technique from our previous system, TIMES, to study surface charge density and biomolecular interaction on the electrode surface.

i-TIMES method is consisted of a microfluidic device with two platinum electrodes embedded in it which are connected to the differential inputs of a transimpedance amplifier. Based on i-TIMES method and the designed experimental process, we are able to quantify the amount of the surface charge density within the electrical double layer at the liquid/solid interface for different buffer strengths, buffer types and pH values. Most uniquely, since i-TIMES signal is generated by the mobile ion or molecule which is not permanently adhered to the electrode surface, the surface molecular coverage can be obtained by comparing the surface charge density on the electrode surface before and after modification. We have measured the surface coverage for thiol-modified single-strand deoxyribonucleic acid (ssDNA) as anchored probe and 6-mercapto-1-hexanol (MCH) as blocking agent on the platinum surface to prove the concept.

In addition, by introducing the biomolecule into the system, we can further demonstrate the effect on surface charge density with different type of biomolecules. The effect of molecular concentration on the surface charge density has been investigated based on various biomolecules including protein (lysozyme and bovine pancreatic ribonuclease A), ligand (N,N’,N″-triacetylchitotriose (TriNAG), p-aminobenzamidine (pABA) and uridine-3'-phosphate(3’-UMP)) and aptamer. Furthermore, the biomolecular interaction can also be determined by analyzing the

change of the surface charge density after interaction based on our own developed i-TIMES physical model.

Overall, our results indicate that the i-TIMES technique is highly sensitive to the physical and chemical properties of buffer and molecules near the electrode surface. Through these experiments, we have demonstrated that i-TIMES method not only can offer a simple and accurate technique to quantify surface charge density on a metal surface but also can be an enabling tool for studies of biomolecular interaction and surface functionalization for biochemical sensing and reactions. Technologically, i-TIMES provides an accurate and convenient tool for quantitative study of surface charge density and molecular interactions without molecular labeling or immobilization. The technique can be attractive to many applications including drug discovery or surface reaction in chemistry.

Chapter 1 Introduction

1.1 Surface Charge Density at the Liquid/Solid Interface

Due to chemical potential difference between a solid surface and a solution, electrical double layer is formed when the solution contacted to any solid surface [1,2]. Electrical double layer is consisted of two layers which are Stern layer and diffusion layer. The ions are absorbed on the atom in the solid more tightly in the Stern layer while it becomes highly mobile in the diffusion layer. The charges in these two layers are countered with each other to assure charge neutrality. The schematic diagram of typical electric double layer is shown in Figure 1.1. Depends on the interaction between charge-charge or charge-dipole, the surface electrical properties can be affected and thus influence the thermodynamics and kinetics of surface reactions.

In many chemical and biomedical applications, surface charge density is always the key question in understanding the surface properties. As a result, the quantification of surface charge density gained much interest and several techniques

have been demonstrated that are capable of quantifying the surface charge density at the liquid/solid interface. To date, Atomic force microscopy (AFM) [3-7], surface plasmonic resonance (SPR) [8,9], streaming potential [10-14] and contact angle titration [15-17] are the most studied techniques which can provide the information about the surface charge density. The schematic diagrams of those techniques are shown in Figure 1.2. To our best knowledge, those techniques have their own limitations and can not directly measure the polarity and the actual amount of surface charge density near the surface which results in limited application in this research field.

To apply AFM to measure surface charge, one measures the force of Coulomb interactions between the AFM tip and the local surface under the tip [3-7]. In this technique, the surface charge density at the liquid/solid interface is obtained by analyzing the electrostatic force as a function of the distance between the tip and the surface. By chemically functionalizing the sample surface, the force between the surface and the AFM tip is changed. Wu *et al*. investigated the force change by different functional molecules such as -Br, -NH_2 and -CH_3 on the surface [3]. The results show a strong relation between the surface charge density and the surface modifications as well as the liquid pH value. Although the AFM technique provides insights about the surface electric properties under different environments, the measurements require sophisticated instrument, have low throughput, rely on detailed information about the tip geometry and its surface charge distribution, and perturb the local environment due to the close proximity of the AFM tip to the surface under test.

Alternatively, SPR technique has been applied to study the effects of surface charge. Shan *et al*. has used electrostatic repulsion between charged particles of the same polarity to balance the gravity in an SPR system [8,9]. Since SPR is sensitive to the refractive index change near a sensor surface, it can be used to measure the equilibrium distance of a particle from the SPR sensor surface. Using the SPR technique, people again show that ionic strength of the solution and surface modifications can change the equilibrium distance between the particle and the surface. However, due to the relatively large size of the particle, the surface properties of the particle itself which can alter the local distributions of the ions in the solution, and difficulties in measuring the distance between the particle and the surface, the SPR technique produces results with relatively large uncertainties and is more suitable for qualitative studies of surface properties in solution [18,19].

There exist also significant efforts to use streaming potential measurements to characterize the surface charge density [10-14]. The technique measures the voltage difference generated by a pressure driven flow over a charged surface or membrane. This measured voltage difference can yield zeta potential. Although one can find the charge density in the diffusion layer from zeta potential, the amount of charge in the diffusion layer is not equal to the total amount of surface charge according to the double layer model. As a result, the streaming potential technique is more suitable for comparing surface properties between different surface modifications. For example, Datta *et al*. has used streaming potential measurement to characterize synthetic membranes with different pore sizes and surface modifications [11]. Kim *et al*. has

applied the technique to show the electric property of a membrane is strongly dependent on the pH value and ionic strength of the solution [12]. In addition to the above methods, people have also measured contact angles to determine the surface charge density at the liquid/solid interface [15-17]. By combining the Young-Lippmann equation with the Guoy-Chapman model for electrical double layer, Horiuchi *et al*. has applied a three-phase contact angle titration measurement to find the dependence of surface potential and surface charge density on the solution pH value [15]. However, since the contact angle is highly sensitive to the surface physical and chemical properties, the contact angle titration measurement is quite complex and difficult to obtain reliable results, and often underestimates the surface charge density.

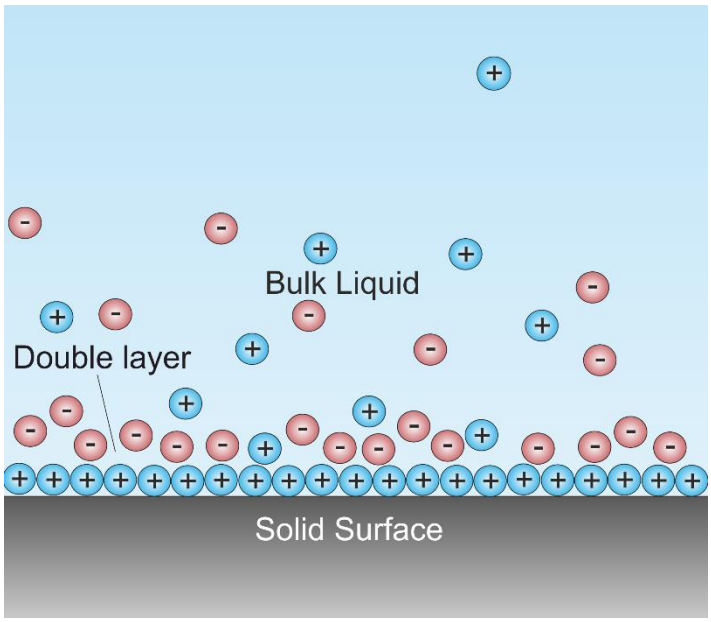

Figure 1.1 The schematic diagram of electric double layer.

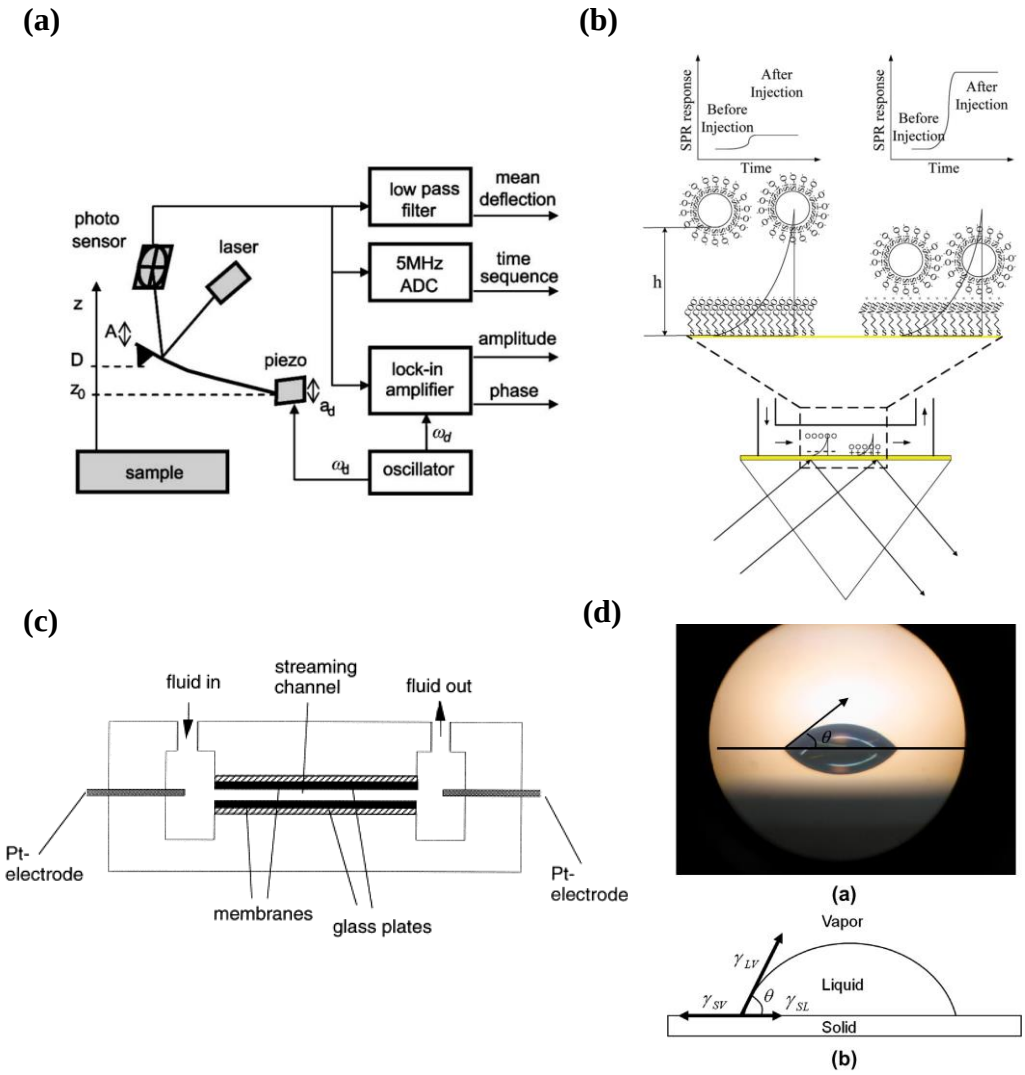

Figure 1.2 The technique for characterization of surface charge density (a) AFM [4], (b) SPR [8], (c) Streaming potential method [14] and (d) Contact angle titration method [15].

1.2 Detection of Protein-Ligand Interaction

Proteins are involved in all the biological process in living cells. Each protein has its own function including cell signaling, structure formation, transportation of ions, and etc. The biological function of the proteins can be inhibited when binding with specific small molecule (i.e. ligands) and change its molecular properties. As a result, to determine the binding affinity between protein with small molecule is an essential question in the field of drug discovery and biomedical process [20,21]. In early stage of drug discovery, hundreds of millions of drug candidates need to be screened. The goal for this screening is to find a potential drug candidate which has high selectivity and high stability to its specific target. Therefore, to find a method that can provide the information about binding affinity between protein and small molecule with high throughput and high reliability is the key to facilitate the drug discovery process.

There are several existing techniques that shows the capabilities to measure the binding affinity of protein and small molecule such as SPR [22-25], isothermal calorimetry (ITC) [26-28], fluorescence resonance energy transfer (FRET) [29-31], biologically modified field effect transistors (BioFET) [32-35] and electrophoretic mobility shift assay (EMSA) [36-38]. Primo *et al*. performed the experiments based on three different nucleic acid-protein complexes by SPR to demonstrate the binding affinity between those biomolecules. From their result, it can be proved that protein and nucleic acids shows similar refractive index increments while binding which determine that no correction is needed for the protein and nucleic acids interaction

when using SPR [23]. Moreover, a single-walled carbon nanotube based BioFET has been used by Melzer *et al*. to investigate the pH and ionic strength effect on the binding between avidin and biotin [33]. Nevertheless, the need of surface modification in SPR and BioFET limit their application since the spatial limitation causes the reaction only occurred nanometer away from the surface. The entropy of the protein-ligand interaction on the surface and in its physiological conditions is much different which affect the accuracy of the experimental result [19,39].

For FRET, Lee *et al*. report an endogenous tryptophan residues and coumarin-derived fluorophore Pacific Blue based FRET method to quantify the binding affinity between small molecules and protein down to nanomolar range [31]. However, the fluorescent labeling on the biomolecule would possibly occupy the active site of the biomolecule and prevent it from interacting with small molecule [40]. Pan et al. modified the original EMSA technique by a high-throughput format which is suitable for small volume samples. They then used the modified EMSA to characterize the binding affinity between a six-member library of recombinant antibodies with enhanced green fluorescence protein (eGFP) [38]. But for EMSA, it requires labeling and detects mobility change of the molecules under an external electric field. The non-equilibrium state of molecules during the electrophoretic process could result in underestimate of the binding affinity [41].

Moreover, ITC, a technique relies on heat releasing of the reaction, shows difficulties in detecting non-covalent complexes which exhibit rather small binding enthalpies. Large sample consumption and low throughput are also its disadvantages

compared to other techniques [42]. It also has difficulties in detecting non-covalent complexes exhibiting rather small binding enthalpy. Figure 1.3 shows the techniques which have been used to determine the binding affinity between protein and ligand.

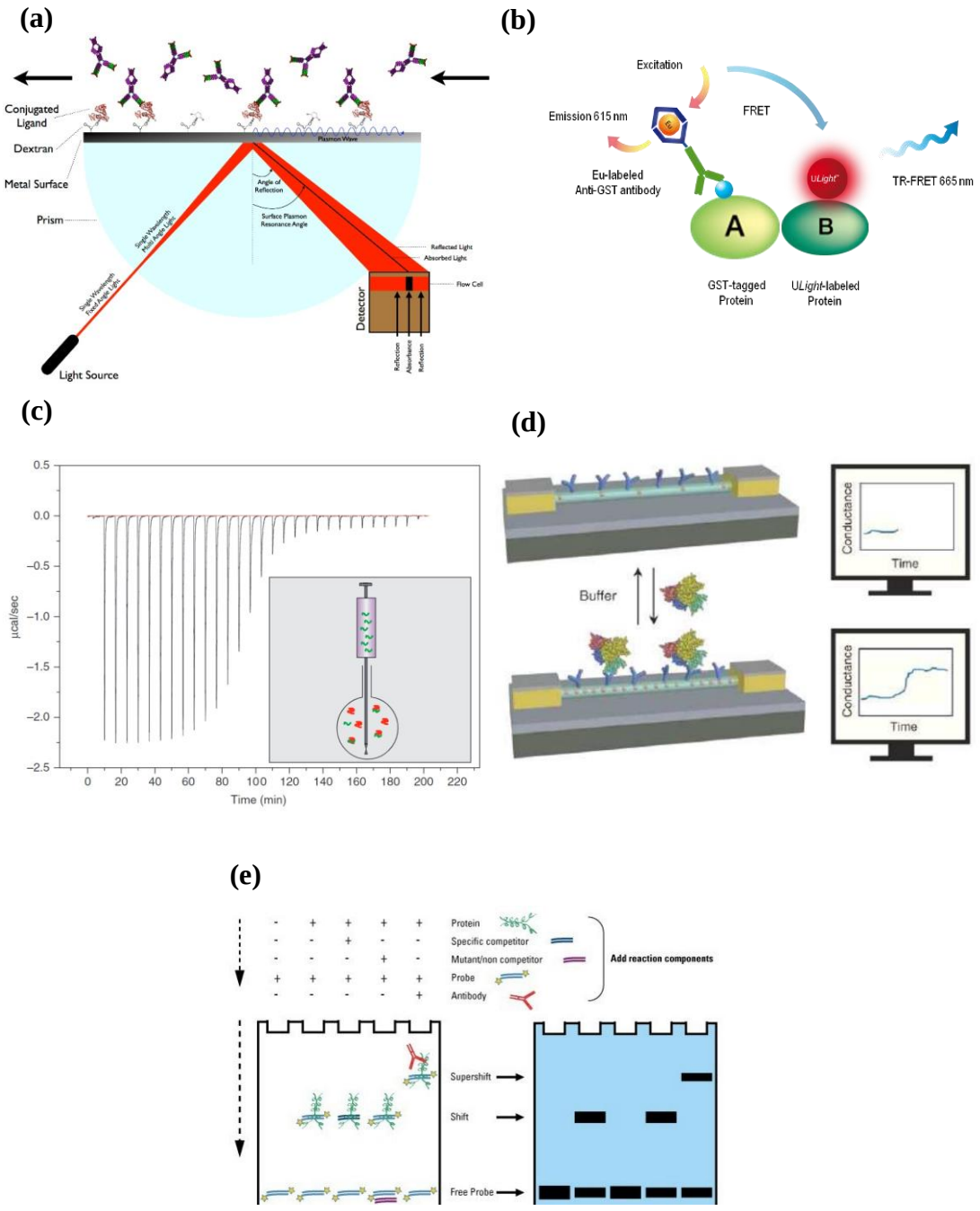

Figure 1.3 The technique for characterization of binding affinty (a) SPR [22-25], (b) FRET [29-31], (c) ITC [28] and (d) BioFET [32-35] and (e) EMSA [36-38].

1.3 Design Motivation of i-TIMES Technique

Different form other techniques mentioned above, the key idea of i-TIMES technique is to offer a label-free, immobilization-free, high throughput and quantitative method which can determine the surface charge density and the molecular interaction near the electrode surface. i-TIMES technique is a modified method from our previous TIMES technique [43,44]. In the previous TIMES technique, the reaction occurs in solution, and the reaction products are brought to an electrode surface via a microfluidic channel. The molecular constituents in the laminar flow approach the electrode by diffusion and induce changes in the surface charge on the electrode surface, generating a transient current that is amplified by a transimpedance amplifier connected to the electrode. By analyzing the transient current signal, the TIMES technique has shown the ability of measuring reaction dissociation constant (K_d). Like the ITC technique, the TIMES method measures the quintessential K_d for reactions in solution. It also has the advantages of high throughput and low reagent consumption in a microfluidic environment. However, later studies found the analysis of transient current signals can suffer from reproducibility problems due to signal-to-noise limits, amplifier bandwidth limit, and external interfaces (e.g. syringe pumps or control valves). Another limit is that the mathematical model used to extract dissociation constant is based on the assumption of superposition, which means the surface concentration of one constituent is not affected by the surface concentration of another constituent. This condition is met only when the overall surface concentration is low or the dwelling time for each molecule (i.e. the amount of time the molecule is in

contact with the electrode surface) is short. Otherwise, the measured reaction dissociation constant can be erroneous. To overcome the limitations, in this dissertation, we have modified the TIMES method by (a) integrating the current signal to obtain the change of surface charge density relative to the surface charge in contact with a reference buffer and (b) measuring the signal when the temporarily adsorbed molecules leave the electrode surface instead of approaching the electrode surface. The former removes the effect of current fluctuations and results in excellent signal-to-noise ratio. The latter improves the measurement reproducibility and controllability since the measurement is made during buffer wash when no molecule of interest is present in the flow, a condition we can confidently establish and repeat. Finally, without analyzing the transient current, the physical model can be simplified without the assumption of superposition. In fact, one can obtain the K_d by visualization of the data without going through detailed models, making the method more intuitively and user friendly.

Similar to TIMES technique, i-TIMES technique is only consisted of a simple design microfluidic device and a transimpedance amplifier which is relatively more easily to fabricated and operated compared to most of the techniques so far. The goal of the dissertation is to determine that i-TIMES technique can not only characterize the surface properties but also reliably detect molecular interaction near the electrode surface.

1.4 Scope of Dissertation

This dissertation discusses the extended development of i-TIMES based on our previous literature [43,44] which can be used to measure the surface charge density at the liquid/solid interface affected by buffer condition or molecular interaction.

In Chapter 2, we will discuss the mechanism and fabrication of the i-TIMES technique. The physical model we developed by our own will also be demonstrated. In Chapter 3, we will determine how the buffer strength, pH value and the buffer type will affect the surface charge density on the electrode surface. In addition to buffer condition, we will also demonstrate how i-TIMES technique can be used to determine the molecular coverage on the surface. Chapter 4 will investigate the biomolecular effect on the surface charge density including protein, aptamer, small ligand and their complexes.

Chapter 2 The Principle of i-TIMES

In this chapter, the i-TIMES device design and fabrication procedure will be discussed. Next, the experimental operation and the analytical model for the i-TIMES technique will be discussed in further detail.

2.1 i-TIMES Device Design and Fabrication Procedure

The i-TIMES system consists of a microfluidic device with two parallel microfluidic channels that are connected to a single channel via a Y-junction. Within each parallel channel that is 1 mm wide and 30 μm high, there is a platinum electrode connected to the external circuit by a bond wire. The electrode area within the channel is 1x1 mm^2. One of the electrodes is used as the sensing electrode and the other as the reference electrode. Both electrodes are connected to the differential inputs of a transimpedance amplifier (TIA) with a tunable transimpedance (Figure 2.1).

To fabricate the i-TIMES device, a 1 mm thick glass substrate was cleaned by acetone, methanol and isopropanol (IPA) in sonication and blown-dried by nitrogen gas. On the glass substrate there are two electrodes with 100 nm titanium (Ti) and 200 nm platinum (Pt) formed by sputtering (Denton Discovery 18, Denton Vacuum, LLC, USA) and photoresist (NR9-1500 PY photoresist) (Futurrex, USA) lift-off process. The 100 nm Ti layer was sputtered in 90 seconds under 200W of power with 35 sccm Argon flow and 2.6 mT chamber pressure. Subsequently, the 200 nm Pt layer was sputtered in 6 minutes under almost the same conditions (200W, 37 sccm Argon flow, 2.9mT chamber pressure). Each Ti/Pt electrode has an area of 1 mm^2 within the microfluidic channel and an extended area outside the channel for wire connection to the external instrument. On the other hand, the microfluidic device contained two 1 mm wide, 30 μm high parallel channels connected to single channel by a Y-junction (Figure 2.1) and was fabricated by soft lithography process. To create the mold for soft lithography, a layer of 30 μm thick SU8-2050 photoresist (Microchem, USA) was formed by UV lithography to create channel patterns. To transfer the patterns from the mold to polydimethylsiloxane (PDMS, Sylgard 184, Dow Corning, USA), uncured PDMS was poured onto the SU8 mold and cured at 65^{o}C for 10 hours. After demolding, fluid inlets and outlets were formed at the end of each channel by hole punching. In the final step of device fabrication, the channel-patterned PDMS and the electrode-patterned glass substrate were bonded together after UV ozone treatment. The detailed fabrication procedure is shown in Figure 2.2. To mount the device onto the system for experiment, the branches connected to the reference electrode and the single channel

of the Y-junction were connected to two syringe pumps (PHD Ultra, Harvard Apparatus, USA) which introduced reference buffer and sample solutions into the microfluidic device.

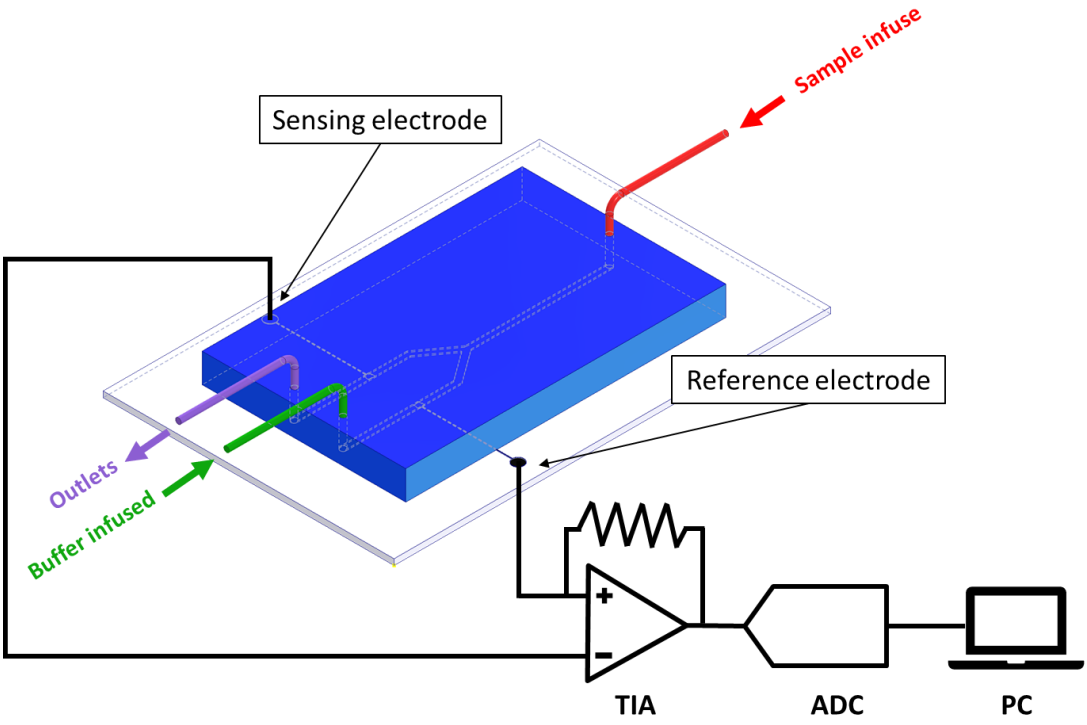

Figure 2.1 The schematic diagram of i-TIMES system set up.

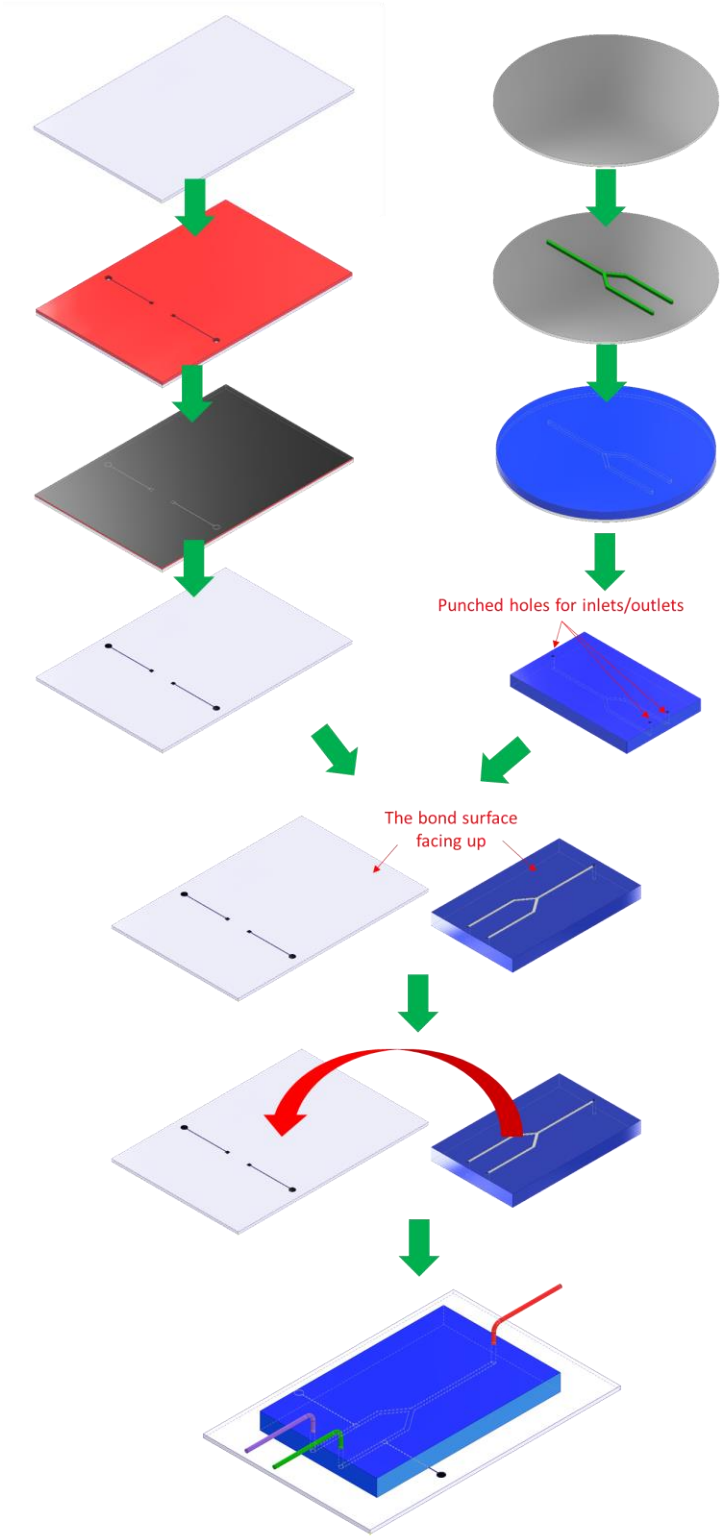

Figure 2.2 The fabrication procedure of i-TIMES device.

2.2 Operation Procedure of the i-TIMES Device

In the beginning of the experiment, the channel with the reference electrode is filled up with reference buffer, and the channel with the sensing electrode is filled up with the sample solution. After soaking each electrode in the respective solution for a sufficient amount of time for the system to reach its steady state, we flow the reference buffer into the channel with the sensing electrode at a flow rate of 100 μL/min so that the sample solution in contact with the sensing electrode is displaced by the reference buffer. We call this step the "washing process" and it is during this "washing process" that the i-TIMES signal is recorded. In other words, we measure the transient current flowing from the sensing electrode into the transimpedance amplifier when the solution above the sensing electrode is switched from the sample solution to the reference buffer. The i-TIMES signal is recorded by connecting both electrode electrically to the differential inputs of a low-noise TIA (SR570, Stanford Research System, Inc, USA). The output voltage of the transimpedance amplifier was connected to a data acquisition (DAQ) board (USB-6251, National Instrument, USA) that digitized the signal. The output from the DAQ board was then recorded by Labview Signal Express under a sampling rate of 1kHz. The typical i-TIMES signal obtained from the "washing process" is shown in Figure 2.3. The polarity of the signal depends on the local buffer condition and molecules within the Debye length.

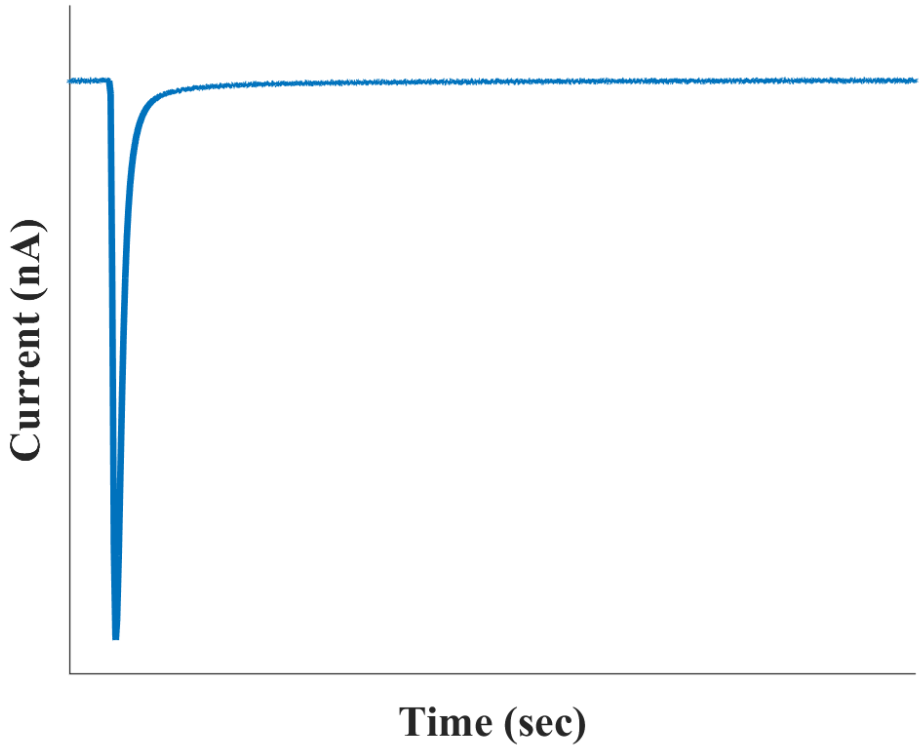

Figure 2.3 Typical i-TIMES signal (Current vs Time).

2.3 Analytical Model of i-TIMES

In this section, a detailed physical model for the biomolecular behavior is presented. The i-TIMES signal produced by different buffer condition and biomolecule (protein, ligand, or protein-ligand complex) are discussed step by step.

2.3.1 Basic Concept of i-TIMES on Surface Charge Density

We can apply the above "washing" procedure to measure the absolute amount and polarity of surface charge for essentially any buffer/electrode combinations. The relative difference in the surface charge density between the sample solution and the reference buffer can be obtained by integrating the i-TIMES current signal over the duration of buffer switching from sample solution to reference buffer. We can obtain the absolute amount of surface charge for the sample solution by choosing a reference buffer that has zero surface charge for a certain electrode. Since we know 0.099 M $KClO_4$/0.001 M $HClO_4$ (pH = 3.4) solution produces zero surface charge with Pt electrode [45], we can use this buffer and another electrode (e.g. Au) to find the surface charge between the buffer and the new electrode material. Similarly, for a given electrode (e.g. Pt), we can also find the surface charge between a new buffer and the electrode by comparing its signal with the signal from the reference (e.g. 0.099 M $KClO_4$/0.001 M $HClO_4$) buffer.

The above process can be described in a simple mathematical formula.

$$S(t) = \int_0^t I(\tau)d\tau = Q_{sample} - Q_{reference} \quad (2-1)$$

where Q_{sample} is the surface charge in the double layer of the sample solution and $Q_{reference}$ is the corresponding quantity for the reference buffer. Equation (2-1) also shows that any permanently adhered molecules do not contribute to the signal since only movable charge produces current. Using this important property, we further demonstrated how the i-TIMES technique can be used to measure surface coverage of molecules anchored to the surface in the later chapter. The surface charge density obtained from the integration of typical i-TIMES signal is shown in Figure 2.4.

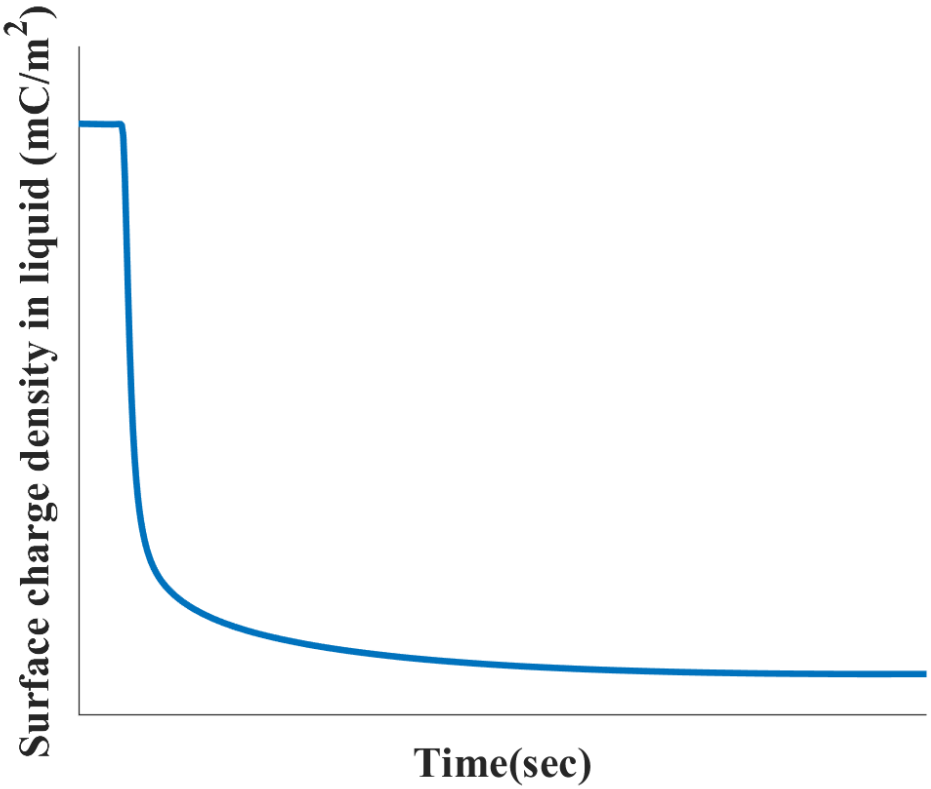

Figure 2.4 The surface charge density obtained from the integration of typical i-TIMES signal (Surface charge density vs Time).

2.3.2 Physical Model of i-TIMES for Biomolecular Interaction

In this section we propose a physical model to describe the relationship between surface charge density and molecular concentration in logarithmic scale. We stress that the measured current signal comes from the mobile charge that leaves the electrode surface during washing. These mobile charges, present in the so-called double layers at the electrode liquid interface, are established when the electrode in the microfluidic channel is immersed in the solution that contains the molecule. When the solution is displaced by the reference buffer, a new equilibrium state between the reference buffer and the electrode is established and the motions of charges in the double layer to establish the new equilibrium state gives rise to the current signal. When integrated, we obtain the total amount of change in surface charge.

We assume that when the electrode is immersed in the solution containing a given kind of molecule, the surface concentration, n_s, and the volume concentration, n, of the molecule follow the relation,

$$n_s = \left(\frac{k_a}{k_d}\right) n e^{-q\zeta/kT} \quad (2-2)$$

where k_a and k_d are the adsorption and desorption coefficients of the molecule at the electrode surface, ζ is the zeta potential, k is Boltzmann constant, T is absolute temperature, and q is the "effective charge" of the molecule. Here effective charge can be different than the actual charge of the molecule in the buffer due to (partial) charge screening (meaning the molecule is "dressed" by ions around it) and the local change in the pH value. Since proton distribution near the liquid/electrode interface is

affected by the potential profile within the Debye length, the molecule at the electrode surface could experience a different local pH value and subsequently, a different charge than it does in the bulk. All these effects determine the effective charge of the molecule near the electrode surface. We further hypothesize that the zeta potential is affected by the surface charge density according to Equation (2-3),

$$\zeta = \zeta_o - \frac{1}{C_T} Q_T \quad (2-3)$$

where Q_T is the change in surface charge, the quantity we measure as i-TIMES signal. C_T is the effective capacitance experienced by Q_T. Equation (2-3) can also be viewed as the first term in the Taylor series expansion of zeta potential over the surface charge density. Physically, we can represent C_T by the series of two capacitances, the capacitance associated with the Debye length and the capacitance due to the (partial) layer deposition of the molecule.

$$\frac{1}{C_T} = \frac{1}{C_D} + \frac{1}{C_M} \sim \frac{1}{C_M} \quad (2-4)$$

We can write $\frac{1}{C_D} = \frac{L_D}{A\epsilon_o\epsilon_{H2O}}$ (A: area of electrode, L_D: Debye length, ϵ_o: permittivity in vacuum, and ϵ_{H2O}: dielectric constant of water) and $\frac{1}{C_M} = \frac{d_M}{A_M\epsilon_o\epsilon_M}$ (A_M: effective area covered by the molecule, d_M: effective thickness of the molecular deposition, and ϵ_M: dielectric constant of molecule). For typical ionic strength of the buffer, $C_D \gg C_M$, thus leading to the approximation in (2-4). We can further model C_M as below

$$C_M = C_{Mo}[\alpha\, u(n_{th} - n) + \beta u(n - n_{th})] \quad when \;\; n > n_o$$

$$= \alpha C_{Mo}\left(\frac{n}{n_o}\right) \quad when \quad n < n_o \quad (2-5)$$

$C_{Mo} = \frac{A\epsilon_o\epsilon_{Mo}}{d_{Mo}}$ is the capacitance of adsorbed molecules over the entire area of electrode. n_o is the concentration above which the linear relation between the surface coverage and the molecular concentration ceases to hold. In most of our measurements, the molecular concentration is actually greater than n_o. u is the unit step function. n_{th} denotes the threshold molecular volume concentration above which the capacitance C_M experiences a sudden change from αC_{Mo} to βC_{Mo}likely due to molecular structural change on the electrode surface (e.g. protein denature or collapse on the metal surface).

Separately, we approximate the relation between Q_T and the surface molecular concentration with Equation (6),

$$Q_T = q' n_s\left(1 - \frac{n_s}{n_{sa}}\right) \quad (2-6)$$

where q' is the change in the surface charge due to departure of a single molecule from the electrode surface. The value or even the sign of q' can be different from the actual charge because ions may take the place left by the molecule and the value of q' depends on the ionic strength, buffer concentration, and pH value of the solution besides the charge of the molecule itself. In other words, q' may not be zero even for a charge neutral molecule because the molecule takes the place that can be otherwise occupied by ions in solution. Here we introduce a parameter, n_{sa}, above which the sign of the signal changed. Part of the reason is that even though we control the pH value of the solution to be constant for solutions of different molecular concentration, the actual pH value (i.e. proton concentration profile) near the electrode surface is

affected by the zeta potential. As zeta potential changes, the "local" pH value changes and this can alter the magnitude and even polarity of the charge contained by the molecule. Hence, we introduce an empirical relation in Equation (2-6) to model this effect. Later on, we will find that the detailed relation in Equation (2-6) will not affect our ability to match the experimental results.

From Equations (2-2) to (2-4), we have

$$n_s \cong \left(\frac{k_a}{k_d}\right) n e^{-\frac{q\zeta_o}{kT}} e^{\frac{qQ_T}{C_M kT}} \quad (2-7)$$

The relation between the surface charge at two different volume concentrations n_1 and n_2 can be represented as

$$\log\left(\frac{n_2}{n_1}\right) = \log\left(\frac{n_{s2}}{n_{s1}}\right) - 0.434\frac{q}{kTC_T}(Q_{T2} - Q_{T1}) \quad (2-8)$$

From Equation (2-6), $Q_T \sim q' n_s \; if \; n_s \ll n_{sa} \quad and \quad Q_T \sim -q'\frac{{n_s}^2}{n_{sa}} \quad if \; n_s \gg n_{sa}$. Therefore,

$$\frac{n_{s2}}{n_{s1}} \sim \frac{Q_{T2}}{Q_{T1}} \; if \; n_{s1,2} \ll n_{sa} \quad or$$

$$\frac{n_{s2}}{n_{s1}} \sim \sqrt{\frac{Q_{T2}}{Q_{T1}}} \; if \; n_{s1,2} \gg n_{sa} \quad (2-9)$$

Substituting Equation (2-9) into Equation (2-8), we obtain

$$\log\left(\frac{n_2}{n_1}\right) = -0.434\frac{q}{kTC_M}(Q_{T2} - Q_{T1}) + \frac{1}{\varphi}\log\left(\frac{Q_{T2}}{Q_{T1}}\right) \quad (2-10)$$

where $\varphi = 1 \; if \; n_{s1,2} \ll n_{sa} \; and \; \varphi = 2 \; if \; n_{s1,2} \gg n_{sa}$.

Since the $\log\left(\frac{Q_{T2}}{Q_{T1}}\right)$ term is much smaller and changes much slowly than the $(Q_{T2} - Q_{T1})$ term unless $Q_{T1}\ and\ Q_{T2}$ are both very small, we can ignore the second term in most cases of our measurements. Then Equation (2-10) can be reduced to Equation (2-11) using the relation in Equation (2-5),

$$\frac{Q_{T2} - Q_{T1}}{\log\left(\frac{n_2}{n_1}\right)} \cong -\alpha \frac{kTC_{Mo}}{2.3q} \equiv P_\alpha\ when\ \ n_o < n_{1,2} < n_{th} \quad (2-11a)$$

$$\frac{Q_{T2} - Q_{T1}}{\log\left(\frac{n_2}{n_1}\right)} \cong -\beta \frac{kTC_{Mo}}{2.3q} \equiv P_\beta\ \ when\ \ n_{1,2} > n_{th} \quad (2-11b)$$

The model describes the piecewise linear characteristics between the surface charge density change and the logarithmic concentration. The detailed on the experimental result will be discussed in later chapter to prove our own developed physical model of i-TIMES.

2.4 Summary

The design idea and fabrication process of the i-TIMES device is illustrated in this chapter, and a physical model is derived to analyze the i-TIMES signal based on the change of surface charge density.

Part of this chapter is a reprint of the material as it appears in *Scientific Reports*, 2019 and *Analytical Chemistry*, 2019. Ping-Wei Chen, Chi-Yang Tseng, Fumin Shi, Bo Bi, Yu-Hwa Lo. Measuring Electric Charge and Molecular Coverage on Electrode Surface from Transient Induced Molecular Electronic Signal (TIMES). *Scientific*

Reports, 2019, 9, 1-10 and Ping-Wei Chen, Chi-Yang Tseng, Fumin Shi, Bo Bi, Yu-Hwa Lo. Detecting Protein-Ligand Interaction from Integrated Transient Induced Molecular Electronic Signal (i-TIMES). *Analytical Chemistry*, 2019, accepted. The dissertation author was the first author of these papers.

Chapter 3 Measuring the Effect of Buffer Condition and Molecular Coverage on Electrode Surface by i-TIMES

In chapter 3, the effect of buffer conditions on electrical charge including ionic strength, pH value and buffer type will be discussed. In addition, the molecular coverage on the electrode surface based on thiol-modified nucleic acid will also be determined from i-TIMES technique

3.1 Overview

Charge density and molecular coverage on the surface of electrode play major roles in the science and technology of surface chemistry and biochemical sensing. However, there has been no easy and direct method to characterize these quantities. By utilizing i-TIMES, we are able to quantify the amount of charge in the double layers at the solution/electrode interface for different buffer strengths, buffer types, and pH values. Most uniquely, such capabilities can be applied to study surface coverage of immobilized molecules. As an example, we have measured the surface coverage for thiol-modified ssDNA as anchored probe and MCH as blocking agent on the platinum surface. Through these experiments, we demonstrate that i-TIMES offers a simple and accurate method to quantify surface charge and coverage of molecules on a metal surface, as an enabling tool for studies of surface properties and surface functionalization for biochemical sensing and reactions.

3.2 Quantification of surface charge density on electrode surface from zero-surface charge buffer.

Since we used 1X PBS as the reference and washing buffer for most of the experiments discussed in the dissertation, we first describe the method of measuring the surface charge density for 1X PBS in contact with the Pt electrode. According to Rizo et al., the solution of 0.099 M KClO4 and 0.001 M HClO4 (pH = 3.4) yields zero-surface charge (ZSC) when it contacts with Pt electrode [45]. Therefore, we can obtain the actual surface charge density for buffer 1X PBS (pH=7.41) by using ZSC

($KClO_4/HClO_4$) as the reference and washing buffer. Following the "washing procedures" described in previous chapter, we obtained the i-TIMES signal (Figure 3.1a) and the surface charge density (Figure 3.1b) using equation (2-1) with 1X PBS being the "sample" and ZSC buffer as the "reference". The result shows that at the 1X PBS/Pt electrode interface, there exists a charge density of 70.67±0.37 mC/m^2 in the electric double layers. For all the experiments in the Chapter 3 where we use 1X PBS as the reference and washing buffer, we will add this amount to the results to obtain the actual amount of surface charge density since our method measures the surface charge difference between the sample solution and the washing buffer.

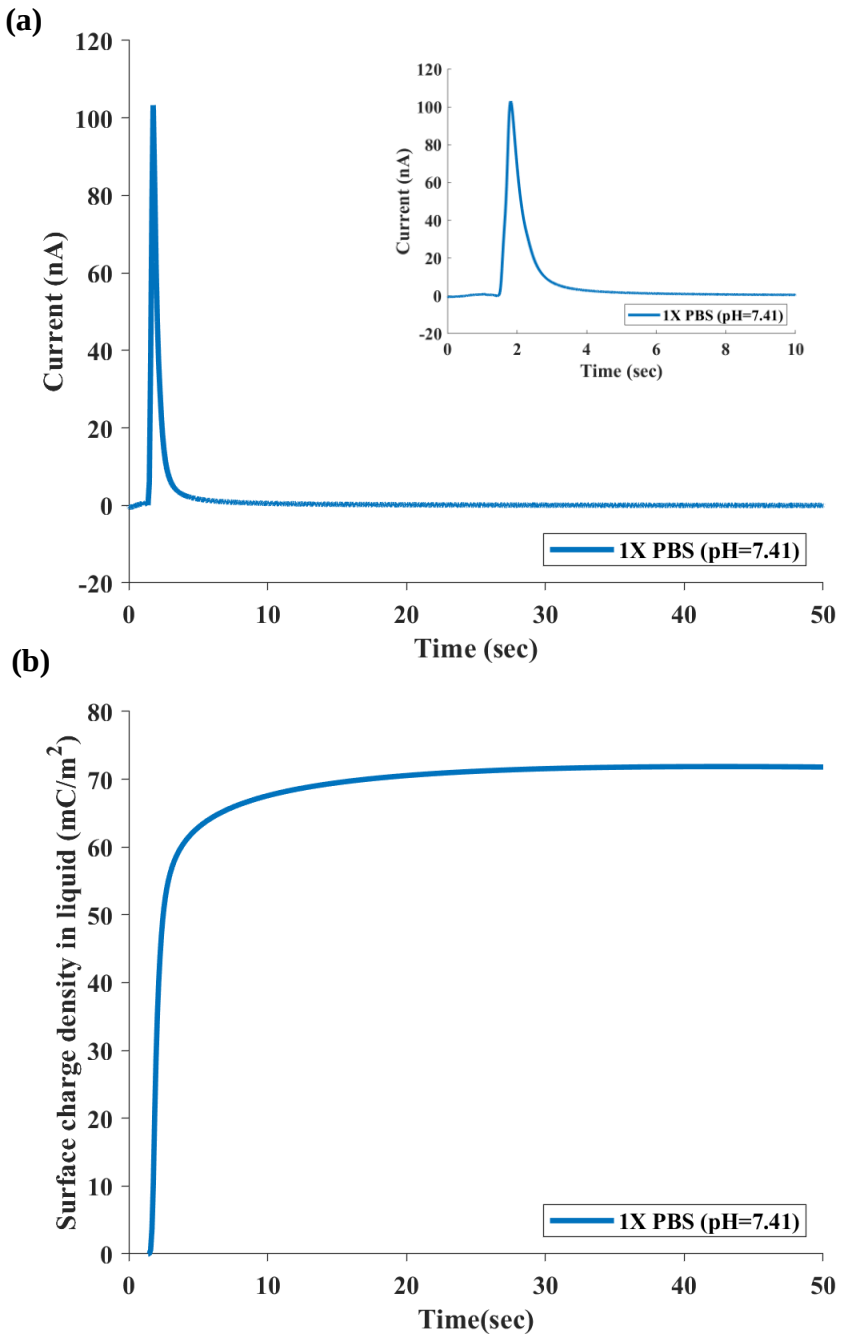

Figure 3.1 i-TIMES signal with 1X PBS on the sensing electrode displaced by the zero-surface charge (ZSC) solution. (a) i-TIMES signal. The inset shows the detailed waveform of the current transient. (b) Change of surface charge density at the solution/solid interface by integration of the -TIMES signal over time. The final value when the system reaches steady state gives rise to the equilibrium surface charge density of the liquid (1X PBS) in contact with a conductive surface (Pt).

3.3 The effect of ionic strength on surface charge density

The i-TIMES signals produced by PBS of different concentration (or ionic strength) are shown in Figure 3.2a. Applying equation (1) with the sample being the PBS of different concentration and the reference (washing buffer) being 1X PBS, we obtain the dependence of surface charge density on the PBS concentration (Figure 3.2b). 1X PBS buffer has its ionic strength (IS) of 162 mM and pH value of 7.41. By varying its ionic strength from 1.6 mM to 1620 mM while keeping the pH value the same (by adding a very small amount of HCl or NaOH that did not alter the ionic strength of the buffer), we have found the following relation between the surface charge density and ionic strength:

$$Q - Q_o = -Q_n \ log\left(\frac{IS}{IS_o}\right), \quad Q_n = 2.59\frac{mC}{m^2} \quad (3-1)$$

It becomes apparent that lower IS produces a greater amount of positive surface charge in the solution in contact with the Pt electrode. However, the effect of IS on the surface charge is rather small since the surface charge density changes from 76.09±0.47 to 68.73±0.06 mC/m^2 when the IS varies by 1000 times from 1.6 mM to 1620 mM.

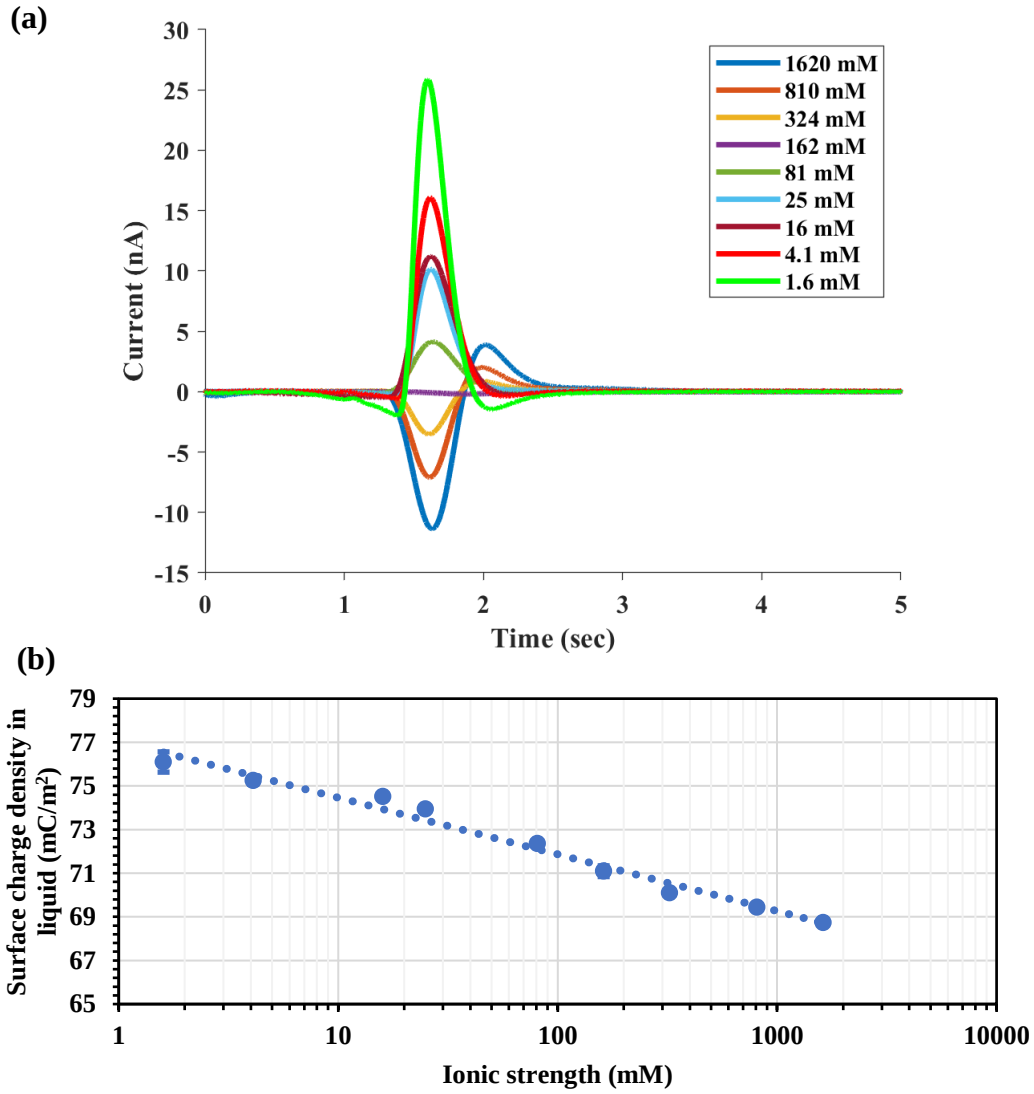

Figure 3.2 i-TIMES signals (a) and surface charge density (b) for different PBS concentration (ionic strength).

3.3 The effect of pH value on surface charge density

The effect of pH value on the surface charge can be obtained following a similar approach. In this study, we have fixed the ionic strength to 1X PBS (162mM) and varied its pH value from 5.69 to 9.65 by adding a small amount of HCl or NaOH. Again, using equation (2-1) with 1X PBS (pH=7.41) being the reference and washing buffer, we have measured the i-TIMES signals (Figure 3.3a) and the surface charge density dependence on the pH value of the buffer (Figure 3.3b). From Figure 3.3b, we can obtain the relation:

$$Q - Q_o = -Q_m \, log\left(\frac{[H^+]}{[H^+]_o}\right), \quad Q_m = 13.67 \frac{mC}{m^2} \quad (3-2)$$

It was found that the surface charge density shows a much stronger dependence on the pH value than the ionic strength. Also, the surface charge density becomes more positive with increasing pH value of the buffer.

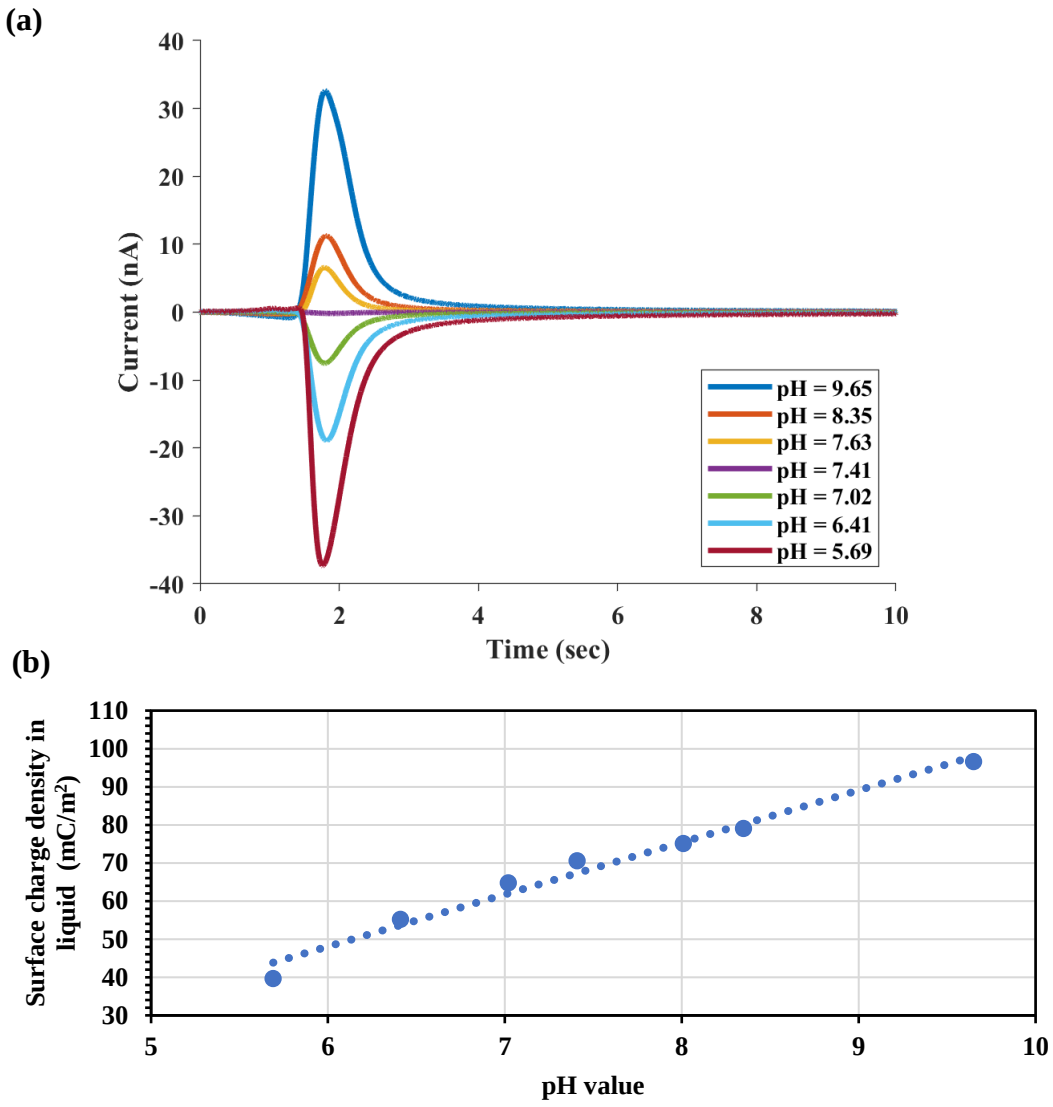

Figure 3.3 i-TIMES signals (a) and surface charge density (b) for different pH value of 1X PBS (IS=162 mM).

3.4 Surface charge density for different buffer types

A biological buffer typically consists of a weak acid and its conjugate base to provide a stable pH environment. We have measured the surface charge for some popular buffer solutions for biological samples, including Tris buffer and HEPES buffer. Figure 3.4 shows the i-TIMES results when we used 25 mM PBS, 25 mM Tris buffer, and 25 mM HEPES buffer as sample solutions and 1X PBS (162 mM, pH=7.41) as the reference and washing buffer at room temperature (25^{o}C). The IS of 25 mM was chosen because it is the preferred concentration for many biological samples. Also noted that for sample solutions under test, we have kept their pH value at their natural state: 7.26 for 25 mM PBS, 7.56 for Tris, and 7.16 for HEPES. After integrating the i-TIMES signals as before, we have found that the actual surface charge density for 25 mM PBS, 25 mM Tris buffer, and 25 mM HEPES buffer are nearly the same: 73.94±0.03, 74.19±0.04 and 75.95±0.04 mC/m^2, respectively.

Next, we found the pH value dependence of surface charge density for each buffer and the results are summarized in Figure 3.5. The i-TIMES signals in Figure 3.5a-c were generated by washing the test samples of different pH value with the same type of 25 mM buffer at its natural pH value (i.e. 7.26 for PBS, 7.56 for Tris buffer, and 7.16 for HEPES buffer). Figure 3.5d shows the pH dependence of surface charge density for all three buffers.

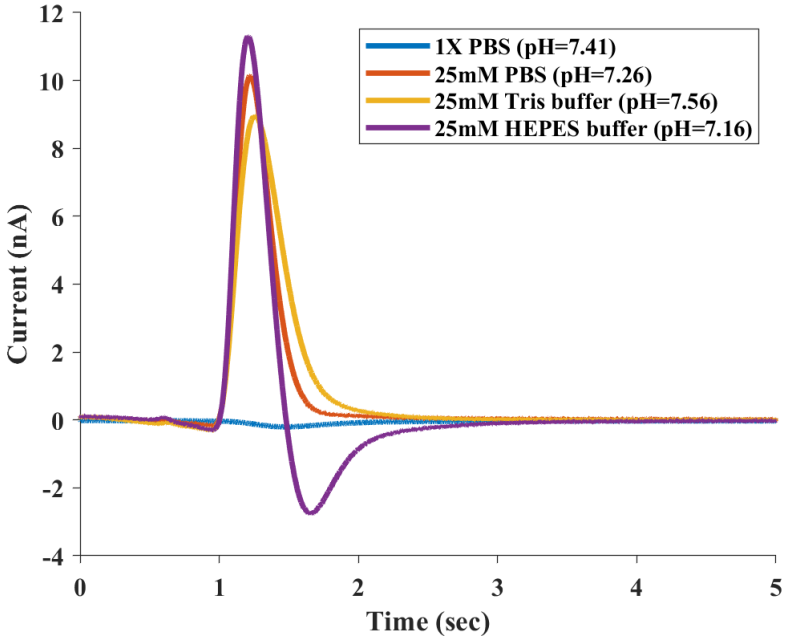

Figure 3.4 i-TIMES signals for 25 mM PBS, 25 mM Tris buffer, and 25 mM HEPES buffer with 1X PBS (162 mM) being the reference and washing buffer.

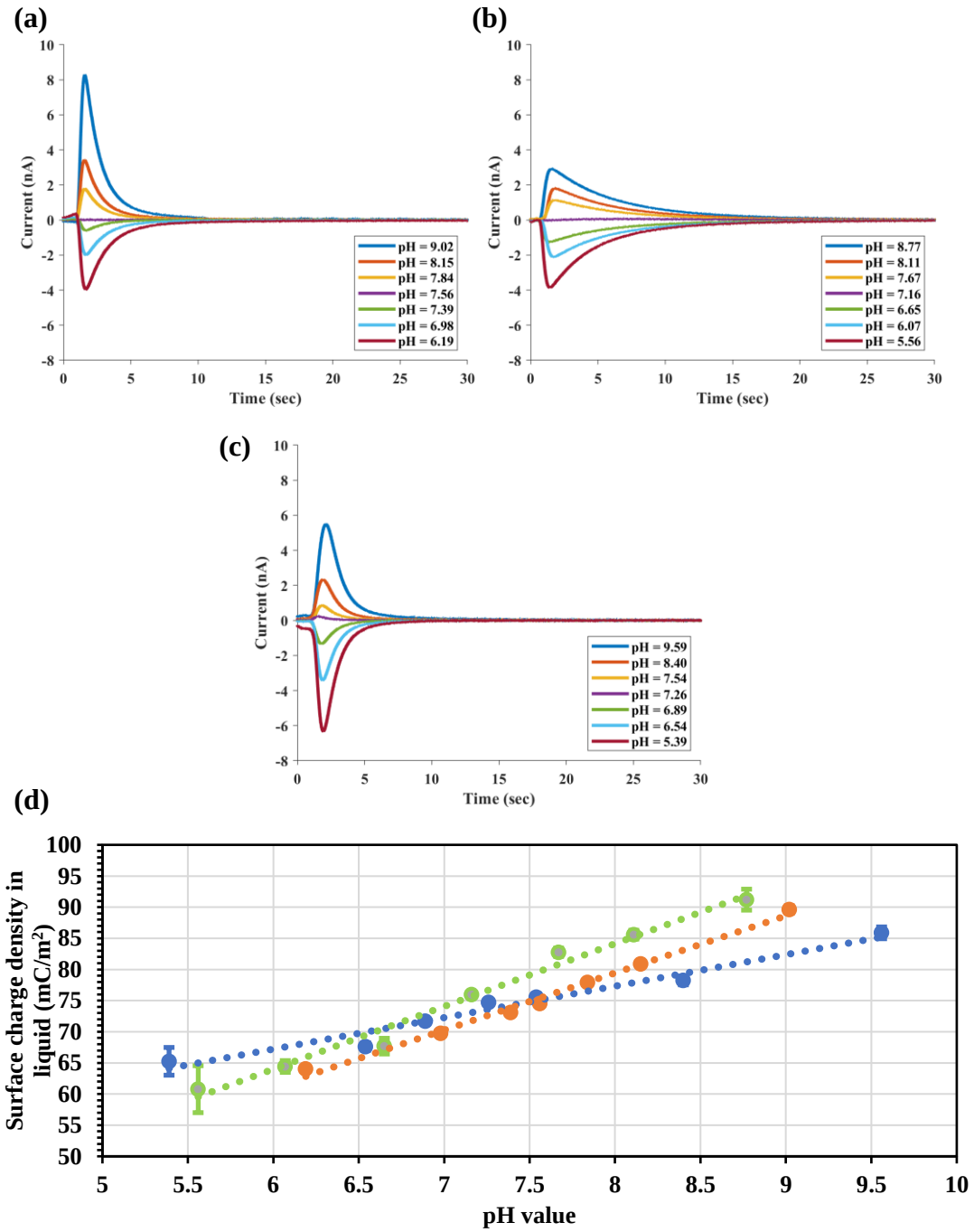

Figure 3.5 i-TIMES signals for 25mM PBS (a), 25mM Tris buffer (b), and 25mM HEPES buffer (c) of different pH value. (d) pH dependence of surface charge density for 25mM PBS (blue), 25mM Tris buffer (orange), and 25mM HEPES buffer (green) buffers.

3.5 Effects of surface modification and surface coverage by immobilized molecules

In this section, we will discuss the effect of surface modification on the surface charge density near the electrode surface by thiol-related molecule. In addition, the determination of surface molecular coverage will also be presented in the section along with the experimental result.

3.5.1 Test strategy

Based on our physical model of i-TIMES, we can measure the effects of surface modification and the fraction of molecular coverage. Here, we have used the concept that any fixed charge created by immobilized molecules on the electrode surface does not contribute to the i-TIMES signal. Therefore, when a fraction of the electrode surface is covered by immobilized molecules, the magnitude of the i-TIMES signals decreases. Provided α be the fraction of surface area covered by a type of molecule bonded to the surface, the surface charge density measured by the i-TIMES signal is expected to be $1-\alpha$ times of signal without surface coverage. Therefore, by taking the ratio of the integrated i-TIMES signal with and without molecular coverage, we can obtain the fraction of molecular coverage after surface modification. The concept is shown in Figure 3.6 which shows that the molecules bonded on the electrode surface will occupy the available site of the mobile ion and results in less detectable surface charge by i-TIMES. Such information is highly valuable because

quantifying the surface coverage by molecules is essential to assure effective surface treatment and repeatable test results for nucleic acid hybridization, immunoassay, particle capturing, and many surface reactions. In our experiment, we used thiol-modified ssDNA and MCH to demonstrate the ability of measuring surface coverage by adherent molecules.

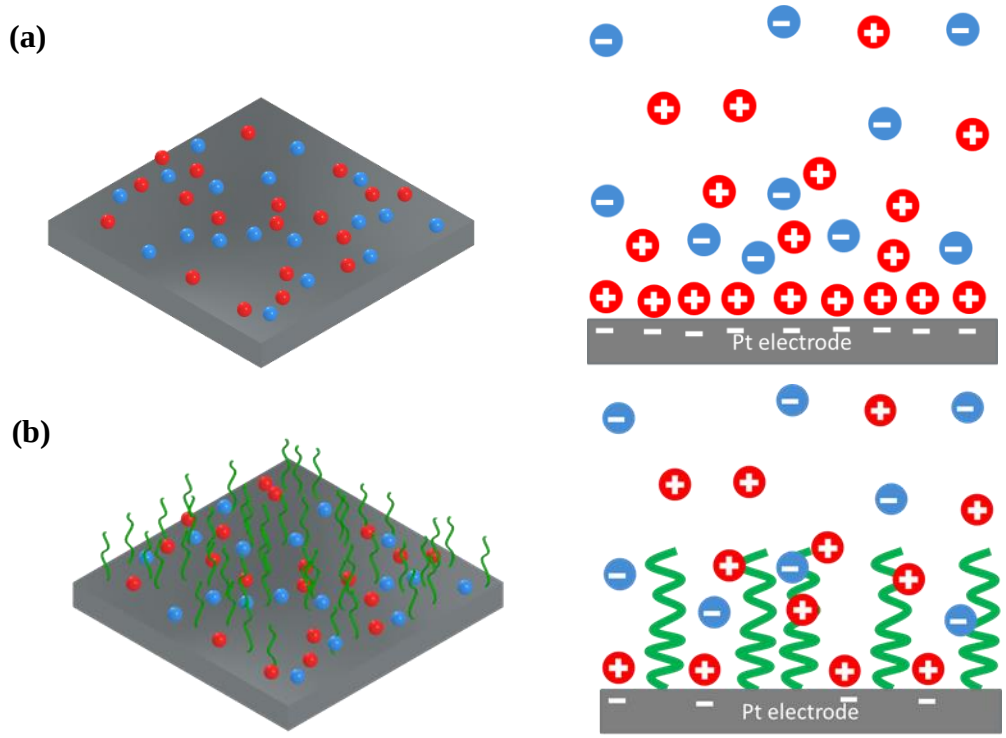

Figure 3.6. The schematic diagram of Pt electrode (a) before the surface modification (b) after surface modification.

3.5.2 Surface modification on Pt electrode

In the experiment of measuring surface coverage, the Pt sensing electrode was modified through sulfur-metal bond. The Pt electrode surface was modified by two types of molecules, MCH (Sigma Aldrich, USA) and thiol-modified ssDNA. The thiol-modified oligos ordered from Integrated DNA Technologies (IDT, USA) were protected by disulfide bond. To reduce the thiol-modified oligos from the disulfide bond, 10 μM oligos solution directly from the stock was mixed with 1 mM dithiothreitol (DTT) in PBS buffer under 4^{o}C for overnight. Afterwards, the mixture went through a Sephadex column to remove DTT. The deprotected oligos solution was then injected into the sensing electrode channel to immobilize ssDNA on the platinum surface via thiol-Pt bonding. The MCH treatment was performed after the ssDNA modification to occupy the surface area uncovered by ssDNA. The MCH treatment was done by filling the same channel with 1 mM MCH in 25 mM PBS for 3 hours. Between each modification, 1X PBS was introduced into the channel at 100 μL/min for 15 mins to remove any unbonded molecule inside the channel.

3.5.3 The surface coverage of MCH

We first tested the surface coverage of MCH as a blocking agent to prevent non-specific binding for sensors of nucleic acid since MCH is supposed to cover any surface area that was not occupied by DNA probes. The sensing electrode in the microfluidic channel was first soaked in 1 mM MCH solution for 3 hours for surface modification. Then the sensing electrode was filled up with 1X PBS with pH=5.69 as

the “sample solution”. When the sample solution was displaced by 1X PBS with pH=7.41, the i-TIMES signal was recorded, as shown in Figure 7a. One can relate surface coverage by MCH to the i-TIMES signal using the following relations:

$$S_1 = Q_{pH5.69} - Q_{pH7.41} \quad (3-3)$$

$$S_2 = (1 - \alpha_{MCH})\left(Q_{pH5.69} - Q_{pH7.41}\right) \quad (3-4)$$

where S_1 and S_2 are the i-TIMES signals with and without MCH surface treatment and α_{MCH} is the fractional area coverage by MCH molecule. From equation (2) and (3), we obtain:

$$\alpha_{MCH} = 1 - \frac{S_2}{S_1} \quad (3-5)$$

Figure 3.7 shows the i-TIMES signals of the above experiment, and the fractional surface coverage for MCH molecule was found to be α_{MCH}=0.943±0.003, as indicated in the first row of Table 3.1. The result shows that 94.3±0.3% of electrode surface area has been covered by MCH as an effective agent to prevent non-specific binding in biosensing.

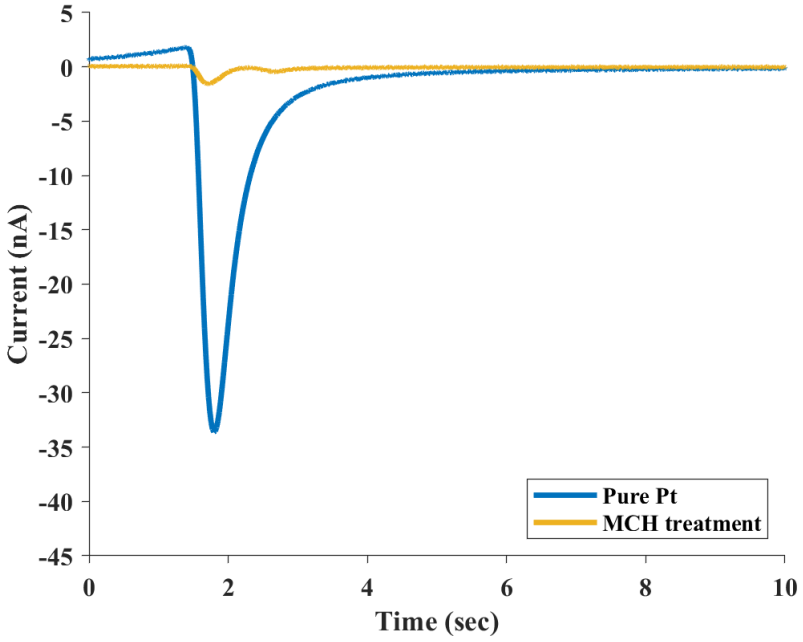

Figure 3.7 i-TIMES signals produced by displacing 1X PBS (pH=5.69) by 1X PBS buffer (pH=7.41) under surface modification of MCH treatment only.

Table 3.1. Fraction of surface coverage by MCH and ssDNA/MCH surface treatments.

Condition	Surface coverage (%)		
	ssDNA	MCH	ssDNA+MCH
1 mM MCH	-	94.3±0.3	-
1 µM ssDNA followed by MCH	48.2±3.3	33.9±3.1	82.2±0.9
10 nM ssDNA followed by MCH	22.6±1.7	69.0±1.6	91.5±0.2
100 pM ssDNA followed by MCH	12.2±0.8	78.8±0.6	91.1±0.7

3.5.4 The surface coverage of thiol-modified ssDNA

Next, we performed experiment with bonding of thiol-modified ssDNA probe of different concentrations (1 μM, 10 nM and 100 pM) to the Pt surface. The ssDNA solution was introduced to the sensing electrode and kept overnight to reach the equilibrium state. Then the channel with the ssDNA treated electrode was filled up with the "sample solution" of 1X PBS with pH=5.69. i-TIMES signals were recorded when the sample solution was displaced by the reference buffer (1X PBS with pH=7.41). Following the measurement, 1 mM MCH was introduced to the ssDNA treated electrode as a blocking agent to cover areas uncovered by ssDNA.

Following the same procedure described previously, we measured i-TIMES signal after MCH treatment. For the ssDNA/MCH treated surface, the signals are expected to follow the relations:

$$S_4 = (1 - \alpha_{ssDNA})\left(Q_{pH5.69} - Q_{pH7.41}\right) \quad (3-6)$$

$$S_5 = (1 - \alpha_{ssDNA} - \alpha_{MCH})\left(Q_{pH5.69} - Q_{pH7.41}\right) \quad (3-7)$$

where S_4 and S_5 are the i-TIMES signals after ssDNA modification and after MCH treatment, respectively. From equation (3-3), (3-6) and (3-7), we can obtain the fractional surface coverage by ssDNA (α_{ssDNA}) and by MCH (α_{MCH}). The i-TIMES signals for different ssDNA concentrations and for the MCH treatment that followed the ssDNA surface modification are shown in Figure 3.8a-c.

The fractional surface coverage by ssDNA and MCH under different conditions is listed in Table 3.1. It was found that when the ssDNA volume concentration changes

from 1μM to 100pM, the surface coverage over the Pt surface changes from 48.2±3.3% to 12.2±0.8%. The results approximately follow the logarithmic relation:

$$\alpha_{DNA} \sim \alpha_{DNAo} log\left(\frac{n_{DNA}}{n_{DNAo}}\right)$$

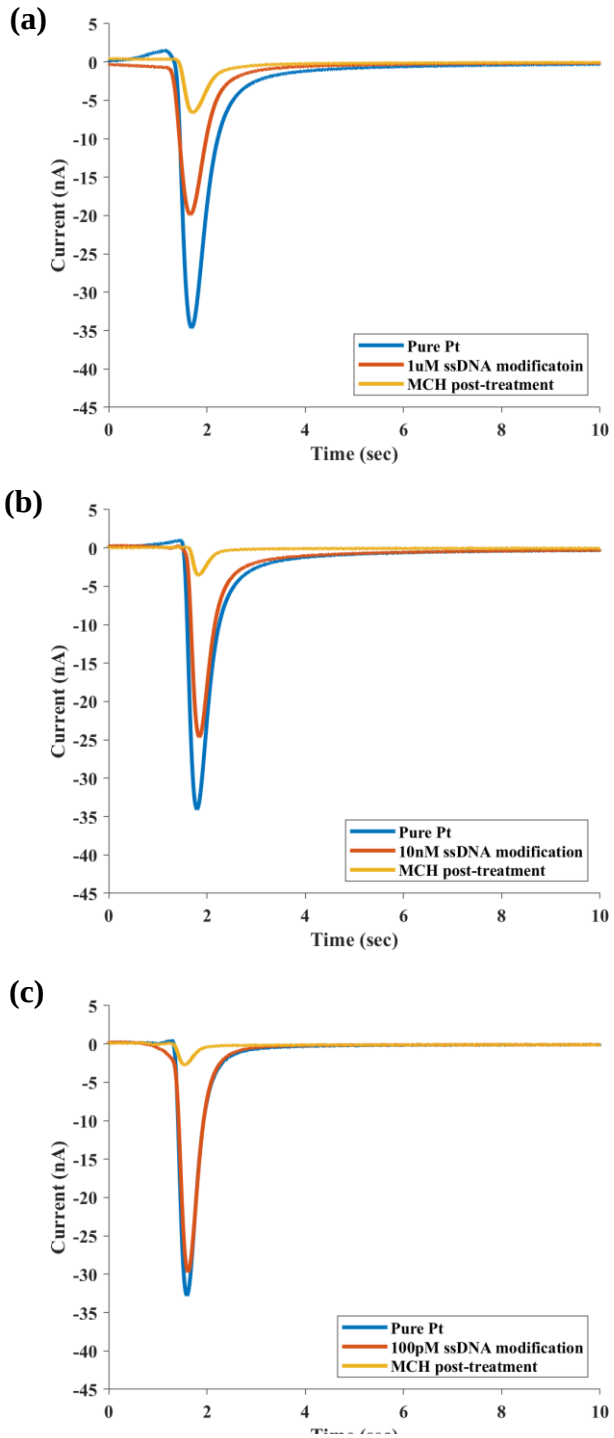

Figure 3.8. i-TIMES signals produced by displacing 1X PBS (pH=5.69) by 1X PBS buffer (pH=7.41) under different surface modification. (a) 1 µM ssDNA modification followed by MCH treatment, (b) 10 nM ssDNA modification followed by MCH treatment (c) 100 pM ssDNA modification followed by MCH treatment.

3.6 Summary

The effect of buffer condition on the surface charge density is presented in this chapter. Moreover, the molecular coverage on the electrode surface by the thiol-modified nucleic acid is also discussed in this chapter. In the next chapter, we will use the same test strategy to determine the molecular interaction effect on surface charge density.

Part of this chapter is a reprint of the material as it appears in *Scientific Reports* 2019. Ping-Wei Chen, Chi-Yang Tseng, Fumin Shi, Bo Bi, Yu-Hwa Lo. Measuring Electric Charge and Molecular Coverage on Electrode Surface from Transient Induced Molecular Electronic Signal (TIMES). *Scientific Reports*, 2019, 9, 1-10. The dissertation author was the first author of this paper.

Chapter 4 Detecting Molecular Interaction Near the Electrode Surface from i-TIMES

In this chapter, the i-TIMES system is used to measure the surface charge density produced by biomolecules such as protein, ligand and aptamer. Moreover, the interaction between protein-ligand/aptamer will be also discussed in this chapter. In this chapter, the result we show is the surface charge density "difference" between the sample solution and the reference buffer which is 1X PBS.

4.1 Overview

Quantitative information about protein-ligand interactions is central to drug discovery. To obtain the quintessential reaction dissociation constant, ideally

measurements of reactions should be performed without perturbations by molecular labeling or immobilization. In this dissertation, we further the development by using i-TIMES to greatly enhance the accuracy and reproducibility of the measurement. While the transient response may be of interest, the integrated signal directly measures the total amount of surface charge density resulted from molecules near the surface of electrode. The i-TIMES signals enable quantitative characterization of protein-ligand interactions. We have demonstrated the feasibility of i-TIMES technique using different biomolecules including lysozyme, N,N',N″-triacetylchitotriose (TriNAG), aptamer, p-aminobenzamidine (pABA), bovine pancreatic ribonuclease A (RNaseA), and uridine-3'-phosphate (3'-UMP). The results show i-TIMES is a simple and accurate technique that can bring tremendous value to drug discovery and research of intermolecular interactions.

4.2 i-TIMES Signal from the Biomolecules and their complexes

As a proof of concept, we have used i-TIMES technique to determine the relationship between the biomolecule concentration and surface charge density. Similar experimental procedure, washing process, was performed for all the experiments based on the biomolecules. In brief, the sample solution was first prefilled into the channel where the sensing electrode locate and the i-TIMES signal was then recorded when it was replaced by the reference buffer which is 1X PBS for all the

experiment. All the pH value of the bio-related solution and buffer was kept at 7.41 by adding a little amount of HCl/NaOH. The related properties obtained from our physical model in chapter 2 are also discussed in this chapter.

4.2.1 Lysozyme, TriNAG and their mixture

Lysozyme is an antimicrobial enzyme that forms part of the innate immune system. TriNAG is an inhibitor which binds to the active site of lysozyme with a dissociation constant (K_d) of 10-30 μM according to literatures [44,46,47]. Figure 4.1a and 4.1b shows the current signal of lysozyme over a concentration range from 0.3nM to 200 μM. Figure 4.1c shows the i-TIMES signals obtained by integrating the current from Figure 4.1a and 4.1b. Each data point in Figure 4.1c is the average of 3 measurements and the variations among measurements are nearly indistinguishable in the plot, showing excellent repeatability. The aforementioned piecewise linear characteristic is clearly shown in Figure 4.1c with two turning points at around 10 nM and 80 μM, respectively.

A similar characteristic can be found from TriNAG. Figure 4.2a and 4.2b show the current signals of TriNAG and TriNAG/lysozyme 1:1 mixture, and Figure 4.2c shows the change of surface charge density with lysozyme, TriNAG, and 1:1 mixture of lysozyme and TriNAG. Again, all the i-TIMES signals show piecewise linear characteristics. Compared with the data from lysozyme and TriNAG alone, the data from the lysozyme/TriNAG mixture sample show a distinct turning point at 10 μM, close to the K_d of the reaction.

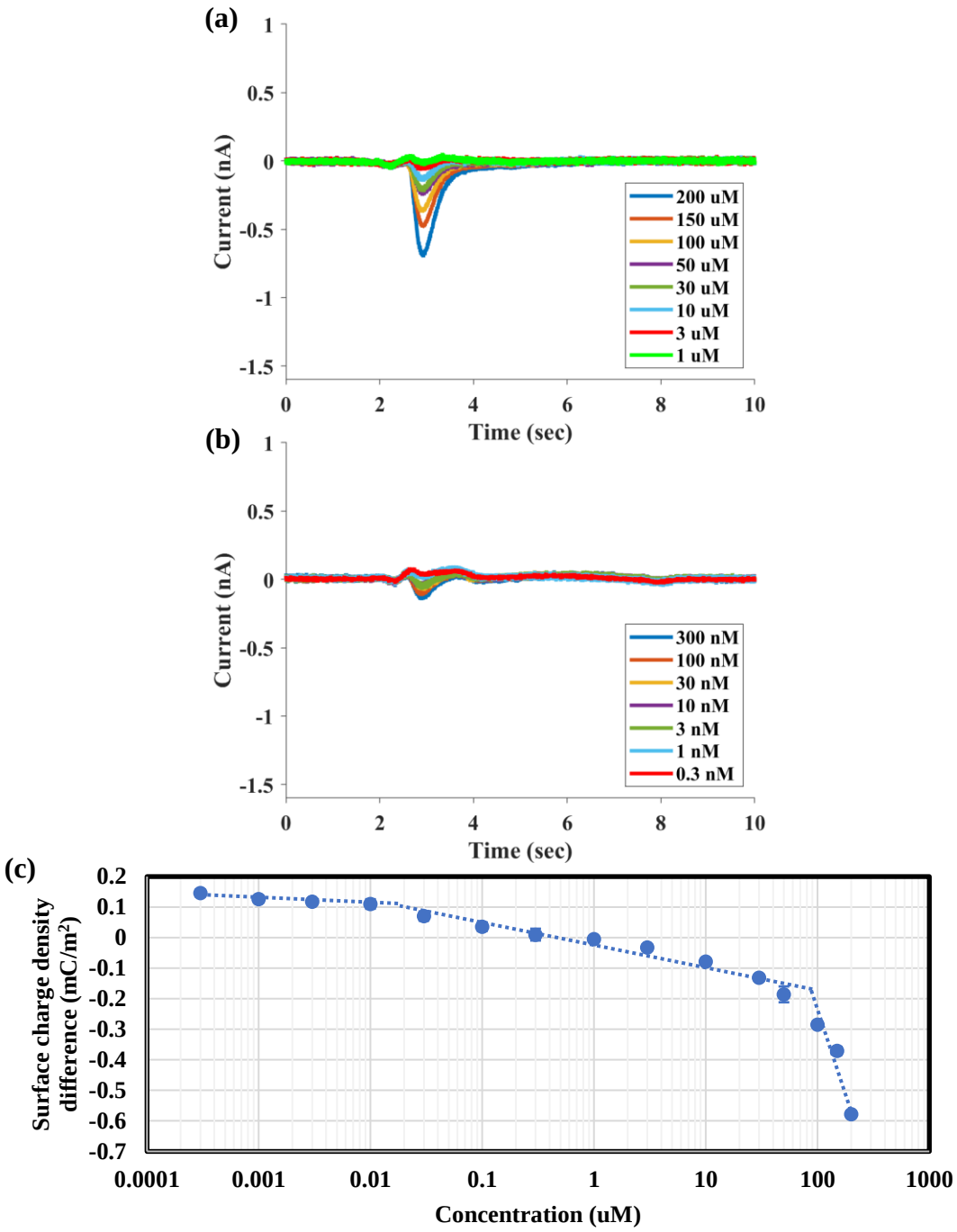

Figure 4.1 i-TIMES signal of (a) Lysozyme (higher concentration), (b) Lysozyme (lower concentration) and (c) dependence of surface charge density on lysozyme concentration (blue). The error bars show the range of 3 measurements.

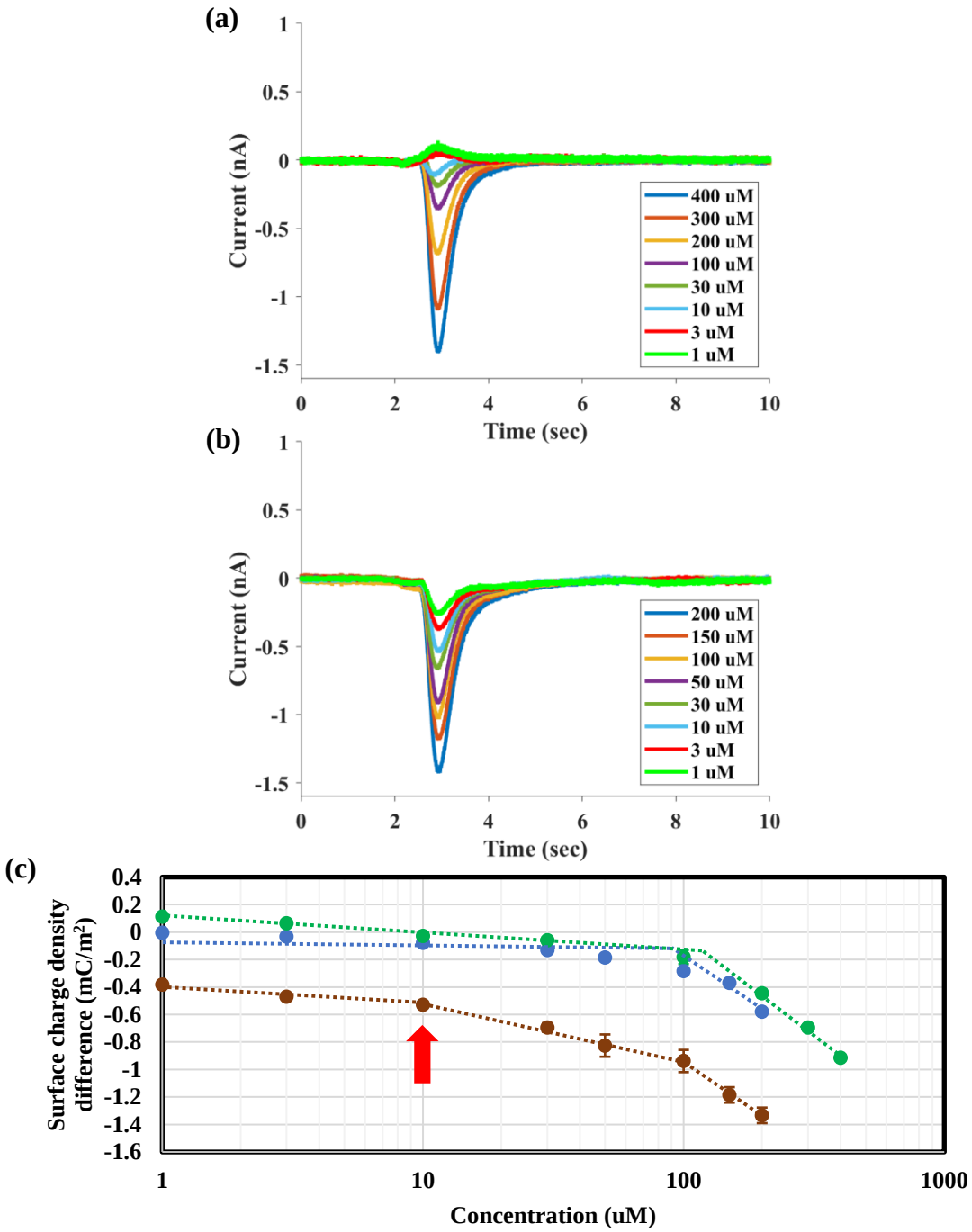

Figure 4.2 i-TIMES signal for (a) TriNAG, (b) 1:1 mixture of TriNAG and lysozyme. (c) Surface charge density of Lysozyme (blue), TriNAG (green) and the TRiNAG/Lysozyme 1:1 mixture (brown). The red arrow indicates the turning point that is approximately equal to the reaction dissociation constant K_d. The error bars show the range of 3 measurements.

4.2.2 Lysozyme, aptamer and their mixture

In another experiment, we applied the i-TIMES method to measure protein-aptamer interaction. Aptamers are ssDNA that can be folded into unique conformations and show high binding affinity to specific target molecule. Using aptamers as ligands for target proteins can be attractive because aptamers can work with a wide range of targets, have high binding affinity and stability, and are easy and inexpensive to produce by polymerase chain reaction (PCR). Literatures have shown several aptamers can react with lysozyme [48]. In our experiment, we used the aptamer sequence GCA GCT AAG CAG GCG GCT CAC AAA ACC ATT CGC ATG CGG C for lysozyme binding, which is reported to produce a K_d of around 3 nM. Figure 4.3a and 4.3b show the current signals for the aptamer molecule alone and the 1:1 mixture of lysozyme and aptamer. The i-TIMES results are plotted in Figure 4.3c. A notable feature for aptamer is that the sign of the current signal is different from the other molecules due to its large density of negative charge. Comparing the i-TIMES data of aptamer, lysozyme, and 1:1 mixture of both, we found that the data of 1:1 mixture follow a similar trend as that of lysozyme, but significantly different from the data of aptamer. However, a closer look at the data of the mixture shows the existence of a new turning point at the concentration of 3 nM, which is very close to the K_d for the lysozyme/aptamer reaction. A zoom-in plot near the turning point of the i-TIMES signal is shown in Figure 4.3d separately.

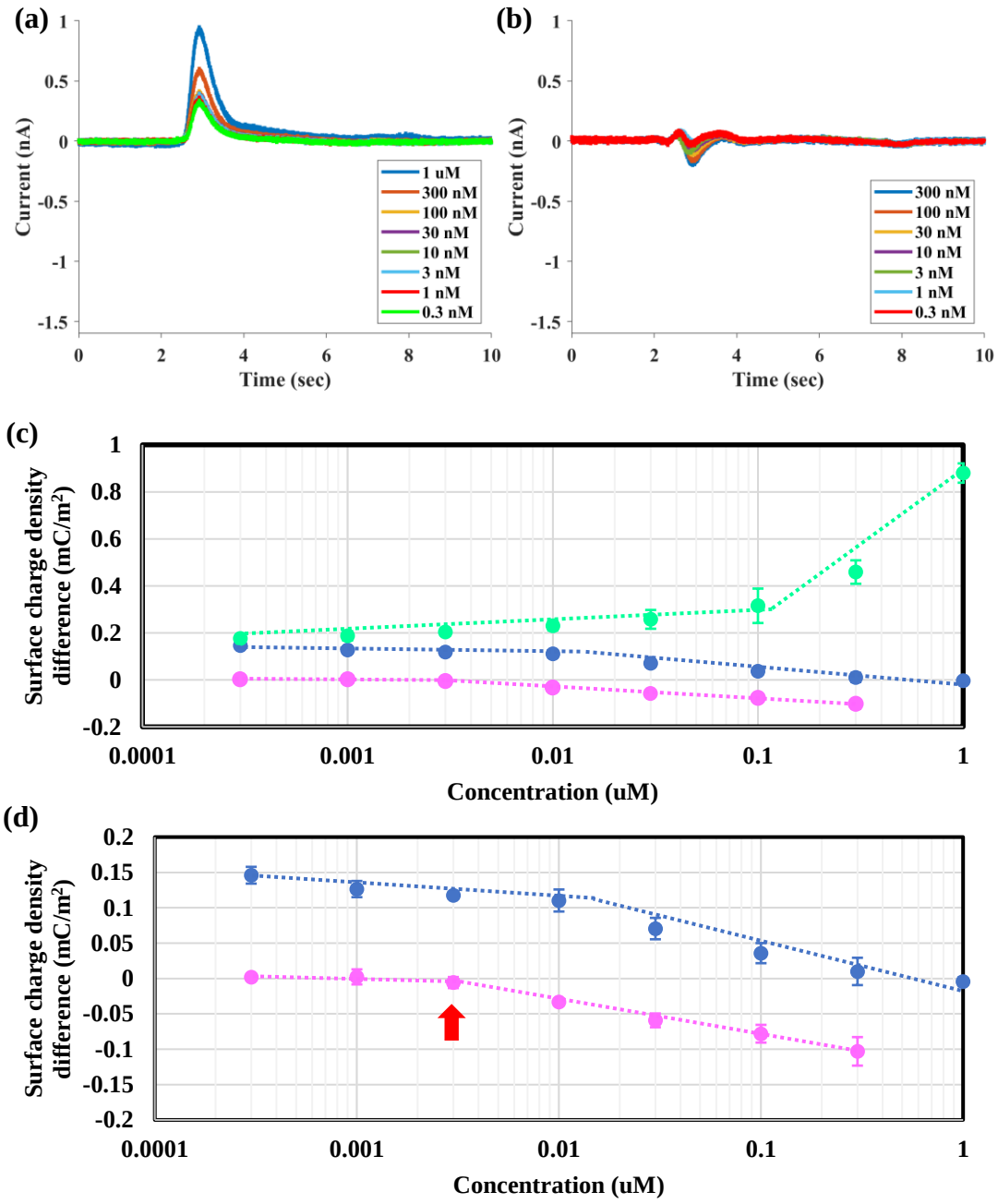

Figure 4.3 i-TIMES signal of (a) Aptamer molecule and (b) 1:1 mixture of aptamer and lysozyme. Note the change of the sign of slope for aptamer because of its large density of negative charge. (c) Surface charge density of Lysozyme (blue), Aptamer (light green) and 1:1 mixture of aptamer and lysozyme (pink). (d) The detailed surface charge density of lysozyme (blue) and 1:1 mixture of aptamer and lysozyme (pink). The red arrow indicates the turning point that is approximately equal to K_d. The error bars show the range of 3 measurements.

4.2.3 Lysozyme, pABA and their mixture

For negative control, we have chosen pABA as the non-reactive ligand to mix with lysozyme. pABA can prevent trypsin from hydrolyzing proteins but does not react with lysozyme. We followed the same procedure to detect the i-TIMES signal of pABA and its 1:1 mixture with lysozyme, and the current signals are shown in Figure 4.4a and 4.4b. After integrating the current signal to obtain the i-TIMES signal, we find the curve of surface charge density for lysozyme and lysozyme/pABA mixture (Figure 4.4c) are very similar, lacking any additional turning point or a slope change as an indicative of the presence of a new molecule. The result shows the absence of enzyme-inhibitor reaction between lysozyme and pABA.

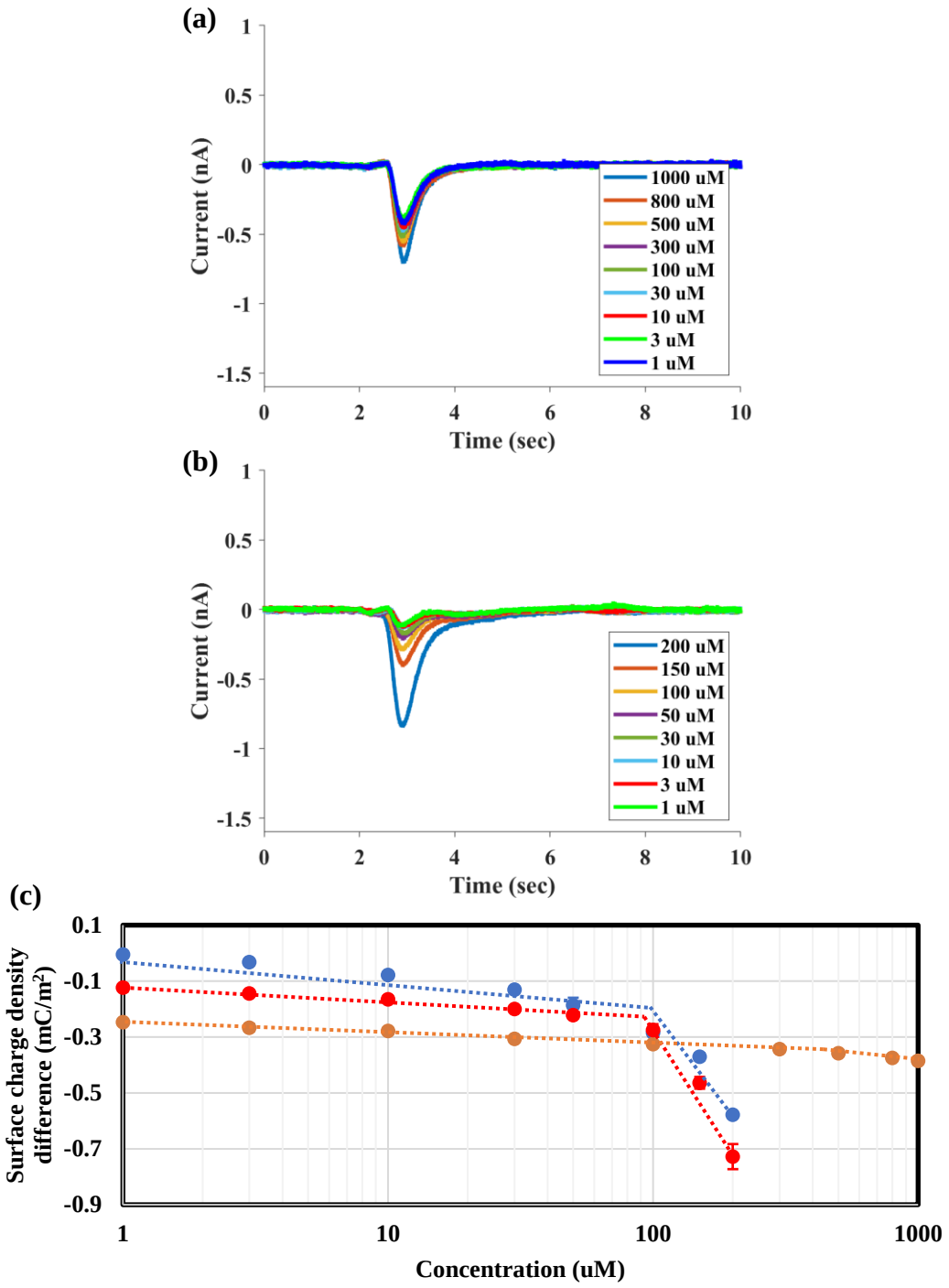

Figure 4.4 i-TIMES signal of molecule (a) pABA (b) 1:1 molar ratio of lysozyme and pABA. (c) Surface charge density of Lysozyme (blue), pABA (orange) and a 1:1 molar ratio of lysozyme and pABA (red).

4.2.4 RNaseA, 3'UMP and their mixture

In another experiment to demonstrate the utility of i-TIMES technique for label-free detection of molecular interactions, we characterized the reaction of RNaseA and its ligand. RNaseA plays an important role in cleaving single-stranded RNA and its property as an enzyme has been studied extensively. The dissociation constant K_d between RNaseA and its ligand, 3'-UMP, has been reported to be 9.7±0.9 μM [49]. The current signals produced by RNaseA, 3'-UMP, and their 1:1 mixture are shown in Figures 4.5a to 4.5c. Similar to the previous experiments, the surface charge density of all the molecules under test displays piecewise linear characteristics with the concentration in logarithmic scale. From Figure 4.5d, an extra turning point for a slope change occurs at 10 μM, which matches well with the published K_d value for RNaseA and 3'-UMP reaction.

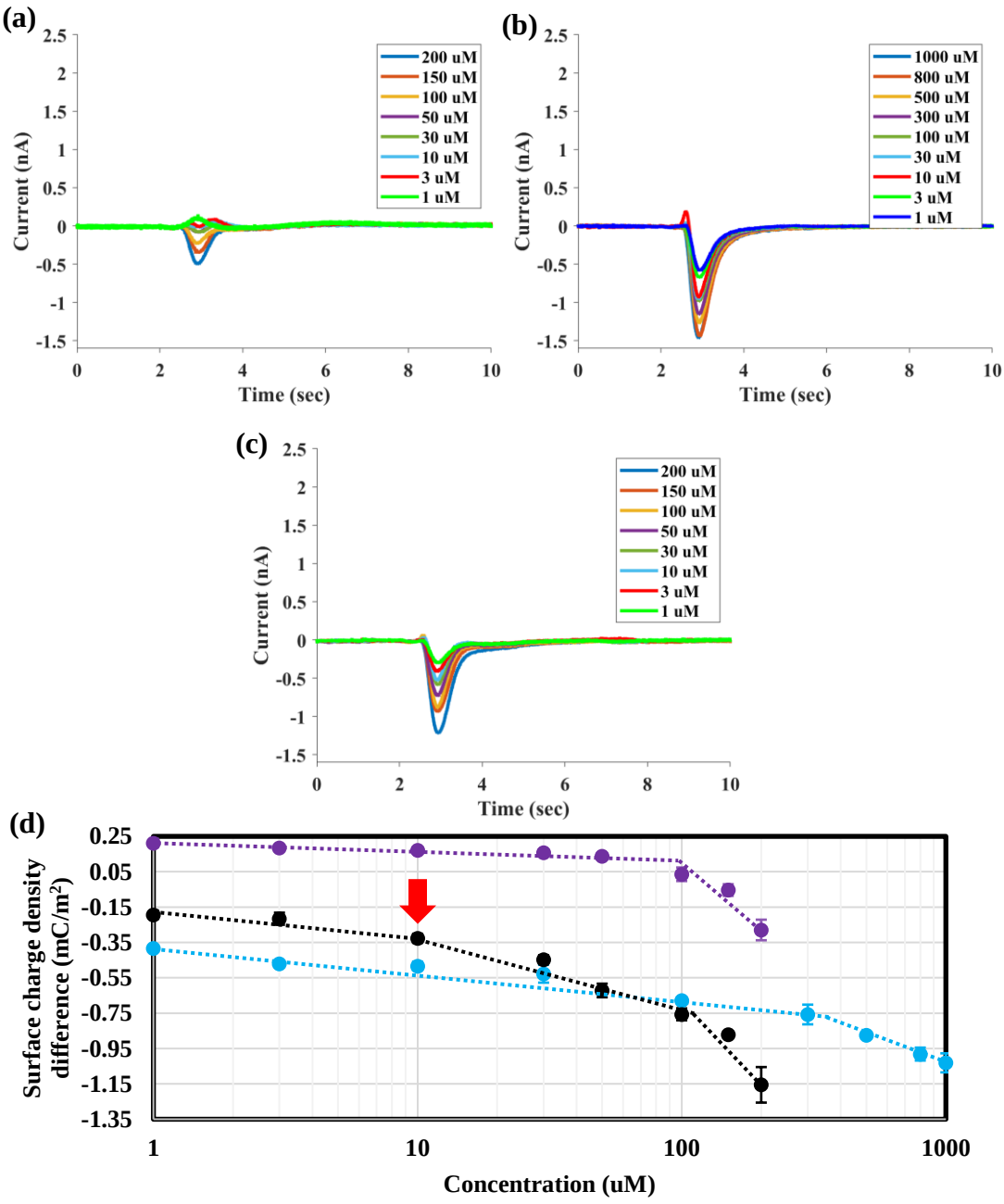

Figure 4.5 i-TIMES signal of molecule (a) RNaseA, (b) 3'-UMP, (c) its complex. (d) Surface charge density of RNaseA (purple), 3'-UMP (light blue) and its complex (black). The red arrow indicates the turning point at the concentration of K_d value.

4.2.5 The parameters obtained from i-TIMES model

Table 4.1 summarized all the parameters obtained from i-TIMES model in chapter 2 which includes P_α, P_β, γ, n_{th} and n_{sa}. To summarize, in a semi-empirical model, we can describe the general behaviors of the i-TIMES signal over a wide concentration range. For each kind of molecule, its i-TIMES signal can be depicted by a set of parameters: $P_\alpha, P_\beta, n_{th}$. The turning point of piecewise linear curve occurs at the concentration n_{th}. All three key parameters in the model can be directly obtained experimentally. When a new type of molecule is present in a significant amount, its features appear in the i-TIMES and are most distinctly represented by the turning points, enabling us to tell the K_d directly from the i-TIMES signal. Finally, observing the ratio of the slopes $\gamma = \frac{P_\beta}{P_\alpha}$ in Table 4.1, we find that the slope ratio, γ, is related to the molecular weight or the size of the molecule. Larger molecules tend to have a greater value of γ, which seems to suggest that when denatured or collapsed to the electrode surface, the effective thickness of the molecule, d_M, decreases and the effective dielectric constant, ϵ_M, increases, causing significant increase in the capacitance in Equation (2-5). Future work with molecular dynamic simulations may provide insight for this interesting trend that seems to provide a good intuitive explanation for the experimental observations from the i-TIMES data.

Table 4.1 Parameters of each molecule obtained from i-TIMES measurements

Molecule	Molecular weight (Da)	P_α (mC/m^2)	P_β (mC/m^2)	$\gamma = \frac{P_\beta}{P_\alpha}$	n_{th} (μM)	n_{sa} (μM)
Lysozyme	14300	-0.09	-1.14	12.67	93.41	0.50
TriNAG	627	-0.15	-1.14	7.60	103.18	5.33
pABA	135	-0.035	-0.11	3.14	325.75	$5.71*10^{-8}$
Aptamer	18587	0.035	0.59	16.86	0.1143	$1.01*10^{-8}$
RNaseA	13700	-0.035	-1.06	30.29	92.08	120.59
3'-UMP	322	-0.16	-0.58	3.63	278.77	0.0058

4.3 Summary

By integrating the transient induced molecular electronic signals, we have demonstrated the i-TIMES technique for label-free, immobilization-free detection of protein-ligand interactions to measure the reaction dissociation constant. To evaluate the viability of the technique, we have used lysozyme-TriNAG and lysozyme-aptamer for positive control while lysozyme-pABA for negative control and RNaseA and 3'-UMP as another set of protein-ligand pair. The results show the existence of clear features in the i-TIMES signal at concentrations that are very close to the reaction K_d.

Portions of this chapter is a reprint of the material as it appears in *Analytical Chemistry*, 2019. Ping-Wei Chen, Chi-Yang Tseng, Fumin Shi, Bo Bi, Yu-Hwa Lo. Detecting Protein-Ligand Interaction from Integrated Transient Induced Molecular Electronic Signal (i-TIMES), *Analytical Chemistry*, 2019, accepted. The dissertation author was the first author of this paper.

Chapter 5 Conclusion

This chapter will provide a brief summary on the material presented in the dissertation and an outlook on the related research directions.

5.1 Summary of Dissertation

This dissertation summarized the extended application of i-TIMES technique. i-TIMES method has been proved to be capable of measuring surface charge density with high signal quality. By using the ZSC solution to the Pt electrode as a reference, we were able to measure the actual value of surface charge density for any chosen buffer suitable for biochemical applications. Using the i-TIMES method and the designed experimental procedures, we have shown quantitatively how the surface charge density is affected by the ionic strength, pH value and type of buffer. Taking advantage of the salient feature that any molecules, charged or not, immobilized on the surface does not contribute to the i-TIMES signal, we have developed schemes to

measure surface coverage for immobilized molecules. We have used thiol-modified ssDNA and MCH molecules as examples to prove the concept.

In addition, i-TIMES has been determined that is able to detect the protein-ligand interaction by analyzing the surface charge density change near the electrode surface. We have used several different protein-ligand pair such as lysozyme-TriNAG (Kd~10-30 μM), lysozyme-aptamer (Kd~3nM), lysozyme-pABA (No reaction) and RNaseA-3'-UMP (Kd~10 μM) to prove the concept. The results clearly show that turning point will be shown up from it piecewise linear curve around the concentration at reaction K_d from i-TIMES which is easily and friendly for the user to prevent any further post data processing. We have also developed a semi-empirical model to elucidate the physical process giving rise to the i-TIMES signal.

Overall, i-TIMES provides a technique with high sensitivity, excellent repeatability and good feasibility which can facilitate the drug discovery process. The label-free, immobilize-free and easy fabrication are the advantages of i-TIMES technique compared to other techniques that makes the result from i-TIMES is more accurate because the properties of molecules will not be affected by any chemical modification. Further application of i-TIMES can be expected since rich information is also contained in the temporal waveform of i-TIMES signal which possibly may provide more insight on the reaction kinetics and charge transport at the solid/liquid interface.

5.2 Outlook

i-TIMES is a promising technique which has the capability to detect the surface properties at the solid/liquid interface by quantification of the surface charge density on the electrode surface. In addition, the molecular interaction can also be detected by i-TIMES technique as long as the surface properties of the molecules are changed. Based on these salient features of i-TIMES, we believe there are several potential applications which can be achieved in the future.

First of all, the material of the electrode in i-TIMES can be replaced such as graphene, carbon nanotube or conductive oxide. For carbon-related material, the excellent electron transfer ability might be beneficial to sensitivity of the i-TIMES technique. In addition, it is relatively easier to modify the surface of carbon-related material by different compound to make it hydrophobic/hydrophilic or positively/negatively charged which can extended the i-TIMES technique to further characterize the surface properties of various type of solid/liquid interface. On the other hand, the transparency of the conductive oxide makes the i-TIMES has possibility to combine with optical readout which makes i-TIMES become promising by compared the result of electrical and optical readout.

Second, in this dissertation, we demonstrate the molecular interaction at steady state which is performed by premixing the molecules for a certain time period before introducing into the i-TIMES system. However, by applying a series of multiple electrodes in a single channel, a change of surface properties during the interaction can be determined by analyzing the surface charge different on each electrode along

the channel. By this way, more insight about reaction kinetic of the molecular interaction can be obtained.

Third, by minimizing the i-TIMES device and integrating it with an analog front-end, the signal-to-noise and the sensitivity can be further improved because it can eliminate the noise due to long cable traces from the sensor to instrument. Therefore, the high sensitivity might lead to a great potential for i-TIMES to detect the surface properties of single molecules.

Last, although we only demonstrate the molecular interaction with a single binding site in this dissertation, it is promising that i-TIMES can be further applied to investigate the interaction which involves multiple binding sites by utilizing different test strategy.

References

1. Grahame, D. The electrical double layer and the theory of electro-capillarity. *Chem. Rev.* **41**, 441-501 (1947)

2. Parsons, R. Electrical double layer: recent experimental and theoretical development. *Chem. Rev.* **90**, 813-826 (1990)

3. Wu, Y., Misra, S., Karacor, M.B., Prakash, S. & Shannon, M.A. Dynamic response of AFM cantilevers to dissimilar functionalized silica surface in aqueous electrolyte solutions. *Langmuir* **26**, 16963-16972 (2010)

4. Wu. Y., Gupta, C. & Shannon, M.A. Effect of solution concentration, surface bias and protonation on the dynamic response of amplitude-modulated atomic force microscopy in water. *Langmuir* **24**, 10817-10824 (2008)

5. Ishino, T., Hieda, H., Tanaka, K. & Gemma, N. Imaging charged functional groups with the atomic force microscope operated in aqueous solutions. *J. Electroanal. Chem.* **438**, 225-230 (1997)

6. Butt, H.J. Measuring local surface charge densities in electrolyte solutions with a scanning force microscope. *Biophys. J.* **63**, 578-582 (1992)

7. Larson, I. & Pugh, R. Qualitative adsorption measurements with an atomic force microscope. *Langmuir* **14**, 5676-5679 (1998)

8. Shan, X., Huang, X., Foley, K.J., Zhang, P., Chen, K., Wang, S. & Tao, N. Measuring surface charge density and particle height using surface plasmon resonance technique. *Anal. Chem*. **82**, 234-240 (2010)

9. Shan, X., Wang, S. & Tao, N. Study of single particle charge and Brownian motions with surface plasmon resonance. *Appl. Phys. Lett.* **97**, 223703 (2010)

10. Molina, C., Victoria, L., Arenas, A. & Ibańez, J. A. Streaming potential and surface charge density of microporous membranes with pore diameter in the range of thickness. *J. Membr. Sci.* **163**, 239-255 (1999)

11. Datta, S., Conlisk, A.T., Kanani, D.M., Zydeny, A.L., Fissell, W.H. & Roy, S. Characterizing the surface charge of synthetic nanomembranes by the streaming potential method. *J. Colloid Interface Sci*. **348**, 85-95 (2010)

12. Kim, K.J., Fane, A.G., Nystrom M., Pihlajamaki, A., Bowen, W.R. & Mukhtar, H. Evaluation of electroosmosis and streaming potential for measurement of electric charges of polymeric membranes. *J. Membrane Sci*. **116**, 149-159 (1996)

13. Afonso, M.D., Hagmeyer, G. & Gimbel, R. Streaming potential measurements to assess the variation of nanofiltration membranes surface charge with the concentration of salt solutions. *Separation/Purification Technology* **22**, 529-541 (2001)

14. Peeters, J.M.M., Mulder, M.H.V. & Strathmann, H. Streaming potential measurements as a characterization method for nanofiltration membranes. *Colloids and Surface A: Physicochem. Eng. Aspects* **150**, 247-259 (1999)

15. Horichi, H., Niolov, A. & Wasan, D.T. Calculation of the surface potential and surface charge density by measurement of the three-phase contact angle. *J. Colloid Interface Sci*. **385**, 218-224 (2012)

16. Hurwitz, G., Guillen, G.R. & Hoek, E.M.V. Probing polyamide membrane surface charge, zeta potential, wettability, and hydrophilicity with contact angle measurements. *J. Membrane Sci*. **349**, 349-357 (2010)

17. Chvedov, D. & Logan, E.L.B. Surface charge properties of oxides and hydroxides formed on metal substrates determined by contact angle titration. *Colloids and Surface A: Physicochem. Eng. Aspects* **240**, 211-223 (2004)

18. Ahmed, F.E., Wiley, J.E., Weidner, D.A., Bonnerup, C. & Mota, H. Surface plasmon resonance (SPR) spectrometry as a tool to analyze nucleic acid-

protein interaction in crude cellular extracts. *Cancer Genomics Proteomics* **7**, 303-310 (2010)

19. Helmerhorst, E., Chandler, D.J., Nussio, M. & Mamotte, C.D. Real-time and label-free biosensing of molecular interactions by surface plasmon resonance: a laboratory medicine perspective. *Clin. Biochem. Rev*. **33**, 161-173 (2012)

20. Drew, J. Drug discover: a historical perspective, *Science*, **287**, 1960-1964 (2000)

21. Neužil, P., Giselbrecht, S., Länge, K., Huang, T.J. & Manz, A. Revisiting lab-on-a-chip technology for drug discovery, *Nat. Rev. Drug Discov.*, **11**, 620-632 (2012)

22. Fagerstam, L.G., Frostell-Karisson, A., Karisson, R., Persson, B. & Ronnberg, I. Biospecific interaction analysis using surface plasmon resonance detection applied to kinetic, binding site and concentration analysis, *J. Chromatogr.*, **597**, 397-410 (1992)

23. Di Primo C. & Lebars, I. Determination of the refractive index increment ratios for protein-nucleic acid complexes by surface plasmon resonance, *Anal. Biochem.*, **368**, 148-155 (2007)

24. Cooper, M.A. Optical biosensors in drug discovery. *Nat. Rev. Drug Discov.*, **1**, 515-528 (2002)

25. Mayer, K.M. & Hafner, J. H. Localized surface plasmon resonance sensors, *Chem. Rev.*, **111**, 3828-3857 (2011)

26. Holdgate, G. Isothermal titration calorimetry and differential scanning calorimetry, *Methods Mol. Biol.*, **572**, 101-33 (2009)

27. Keller, S., Vargas, C., Zhao, H., Piszczek, G., Brautigam, C.A. & Schuck, P. High-precision isothermal titration calorimetry with automated peak shape analysis, *Anal. Chem.*, **84**, 5066-5073 (2012)

28. Leavitt, S. & Freire, E. Direct measurement of protein binding energetics by isothermal titration calorimetry, *Biophys. Methods*, **11**, 560-566 (2001)

29. Endoh, T., Funabashi, H., Mie, M. & Kobatake, E. Method for detection of specific nucleic acids by recombinant protein with fluorescent resonance energy transfer, *Anal. Chem.*, **77**, 4308-4314 (2005)

30. Mocz, G. & Ross, J.A. Fluorescence techniques in analysis of protein-ligand interactions, *Methods mol. Biol.*, **1008**, 169-210 (2013)

31. Lee, M.M. & Peterson, B.R. Quantification of small molecule-protein interactions using FRET between tryptophan and the pacific blue fluorophore, *ACS Omega*, **1**, 1266-1276 (2016)

32. Schöning, M. J. & Poghossian, A. Recent advances in biologically sensitive field-effect transistors (BioFETs). *Analyst*, **127**, 1137-1151 (2002)

33. Munzer, A.M., Seo, W., Morgan, G.J., Michael, Z.P., Zhao, Y., Melzer, K., Scarpa, G. & Star, A. Sensing reversible protein-ligand interactions with single-walled carbon nanotube field-effect transistors, *J. Phys. Chem. C*, **118**, 17193-17199 (2014)

34. Star, A., Gabriel, J.C.P., Bradley, K. & GrUner, G. Electronic detection of specific protein binding using nanotube FET devices, 2003, *Nano Letter*, **3**, 459-463 (2003)

35. Maehashi, K., Katsura, T., Kerman, K., Takamura, Y., Matsumoto, K. & Tamiya, E. Label-free protein biosensor based on aptamer-modified carbon nanotube field-effect transistors, *Anal. Chem.*, **79**, 782-787 (2007)

36. Garner, M.M. & Revzin, A. A gel electrophoresis method for quantifying the binding of proteins to specific DNA regions: application to components of the Escherichia coli lactose operon regulatory system. *Nucleic Acids Res*., **9**, 3047-3060 (1981)

37. Pan, Y., Duncombe, T.A., Kellenberger, C.A., Hammond M.C. & Herr, A.E. High-throughput electrophoretic mobility shift assays for quantitative analysis of molecular binding reactions. *Anal. Chem*., **86**, 10357-10364 (2014)

38. Pan, Y., Sackmann, E.K., Wypisniak K., Hornsby, M., Datwani S.S. & Herr, A.E. Determination of equilibrium dissociation constants for recombinant antibodies by highthroughput affinity electrophoresis. *Sci. Reports*, **6**, 39774 (2016)

39. Ahmed, F.E., Wiley, J.E., Weidner, D.A., Bonnerup, C. & Mota, H. Surface plasmon resonance (SPR) spectrometry as a tool to analyze nucleic acid-protein interactions in crude cellular extracts, *Cancer Genomics & Proteomics*, **7**, 303-310 (2010)

40. Preus, S. & Wilhelmsson, L.M. Advances in quantitative FRET-based methods for studying nucleic acids, *ChemBioChem*, **13**, 1990-2001 (2012)

41. Hellman, L.M. & Fried, M.G. Electrophoretic mobility shift assay (EMSA) for detecting protein-nucleic acid interactions. *Nat. Protoc.*, **2**, 1849-1861 (2007)

42. Du, X., Li, Y., Xia, Y.L., Ai, S.M., Liang, J., Sang, P., Ji, X.L. & Liu, S.Q. Insights into protein-ligand interactions: mechanisms, models, and methods, *Int. J. Mol. Sci.*, **17**, 144 (2016)

43. Zhang, T., Ku, T.H., Han, Y., Subramanian, R., Niaz, I.A., Luo, H., Chang, D., Huang, J.J. & Lo, Y.H. Transient induced molecular electronic spectroscopy (TIMES) for study of protein-ligand interactions. *Sci. Reports*, **6**, 35570 (2016)

44. Zhang, T., Wei, T., Han, Y., Ma, H., Samieegohar, M., Chen, P.W., Lian, I. & Lo, Y.H. Protein-ligand interaction detection with a novel method of transient induced molecular electronic spec-troscopy (TIMES): Experimental and theoretical studies. *ACS Cent. Sci.*, **2**, 834-842 (2016)

45. Rizo, R., Sitta, E., Herrero, E., Climent, V. & Feliu, J.M. Towards the understanding of the interfacial pH scale at Pt (1 1 1) electrodes. *Electrochim. Acta* **162**, 138-145 (2016)

46. Svobodova, J., Mathur, S., Muck, A., Letzel, T. & Svatos, A. Microchip-ESI-MS determination of dissociation constant of the lysozyme-NAG_3 complex. *Electrophoresis*, **31**, 2680−2685 (2010)

47. Jecklin, M. C., Touboul, D., Bovet, C., Wortmann, A. & Zenobi, R. Which electrospray-based ionization method best reflects proteinligand interactions found in solution? a comparison of ESI, nanoESI, and ESSI for the determination of dissociation constants with mass spectrometry. *J. Am. Soc. Mass Spectrom.*, **19**, 332-343 (2008)

48. Tran, D.T., Janssen, K.P.F., Pollet, J., Lammertyn, E., Anne, J., Schepdael, A.V. & Lammertyn, J. Selection and characterization of DNA aptamers for egg white lysozyme, *Molecules*, **15**, 1127-1140 (2010)

49. Doucet, N., Jayasundera, T.B., Simonovic, M. & Loria, J.P. The crystal structure of ribonuclease A in complex with thymidine-3'-monophosphate provides further insight into ligand binding, *Proteins*, **11**, 2459-68 (2010)